

# Tailoring Polymer-Based Nanoassemblies for Stimuli-Responsive Theranostic Applications

Moritz S. Muthwill, Phally Kong, Ionel Adrian Dinu, Danut Necula, Christoph John, and Cornelia G. Palivan\*

Dedicated to the memory of Prof. Wolfgang Meier (1964–2022)

Polymer assemblies on the nanoscale represent a powerful toolbox for the design of theranostic systems when combined with both therapeutic compounds and diagnostic reporting ones. Here, recent advances in the design of theranostic systems for various diseases, containing—in their architecture—either polymers or polymer assemblies as one of the building blocks are presented. This review encompasses the general principles of polymer self-assembly, from the production of adequate copolymers up to supramolecular assemblies with theranostic functionality. Such polymer nanoassemblies can be further tailored through the incorporation of inorganic nanoparticles to endow them with multifunctional therapeutic and/or diagnostic features. Systems that change their architecture or properties in the presence of stimuli are selected, as responsivity to changes in the environment is a key factor for enhancing efficiency. Such theranostic systems are based on the intrinsic properties of copolymers or one of the other components. In addition, systems with a more complex architecture, such as multicompartments, are presented. Selected systems indicate the advantages of such theranostic approaches and provide a basis for further developments in the field.

to image that specific region. The dual functionality of theranostic systems represents a powerful tool in decreasing the discomfort associated with separate medical treatments and imaging approaches. In addition, the encapsulated imaging components serve to distinguish where exactly the system is located, increasing the efficiency of the therapeutic compound and decreasing side effects. In this respect, the use of nanoassemblies has revolutionized the field due to their capability to be up-taken without affecting the surrounding healthy tissue, and hence, allowing a reduction of the biological side effects. Theranostic systems with nanometer sizes have been reported for the treatment of various diseases, including cancer,<sup>[1–6]</sup> brain diseases,<sup>[7,8]</sup> cardiovascular diseases,<sup>[9–12]</sup> deficiencies due to genetics,<sup>[13]</sup> lung diseases,<sup>[14]</sup> atherosclerosis,<sup>[15,16]</sup> rheumatoid arthritis,<sup>[15]</sup> and visceral leishmaniasis, caused by intracellular protozoan parasites of *Leishmania* genus.<sup>[17]</sup>

## 1. Introduction

Theranostics is an emerging field that elegantly combines both therapy and diagnosis, i.e., it acts on a specific site for the treatment of a pathologic condition and simultaneously provides ways

A particularly appealing class of carriers developed to support theranostic approaches is based on polymer assemblies, structures including nanoparticles (NPs), micelles, and vesicles. Various properties of polymeric nanoassemblies, such as size, shape, and surface chemistry, play an important role in the circulation throughout the body, specific organ distribution, and specific cell uptake.<sup>[18,19]</sup> Vesicles, nanoparticles, and macromolecules of a certain size tend to accumulate at the tumor site through passive targeting via the enhanced permeability and retention (EPR) effect.<sup>[20–22]</sup> For example, nanoparticles with a size below 5 nm do not remain in the blood stream and are eliminated by extravasation or renal clearance, while larger nanoparticles (near-micrometer range and above) accumulate in the liver and spleen.<sup>[23]</sup> A second molecular factor influencing the in vivo carrier efficiency is its surface chemistry because it influences the biodistribution. In this respect, polymer coatings serve to stabilize the nanoparticles and increase their dispersion in blood circulation.<sup>[18,19]</sup> The impact of the shape of nanoparticles on their fate inside the body was shown, for example, by PEGylated gold nanospheres, which had a longer half-life in the blood stream, a lower clearance by the reticuloendothelial system, and a higher overall tumor uptake than the disk-, rod- or cage-shaped

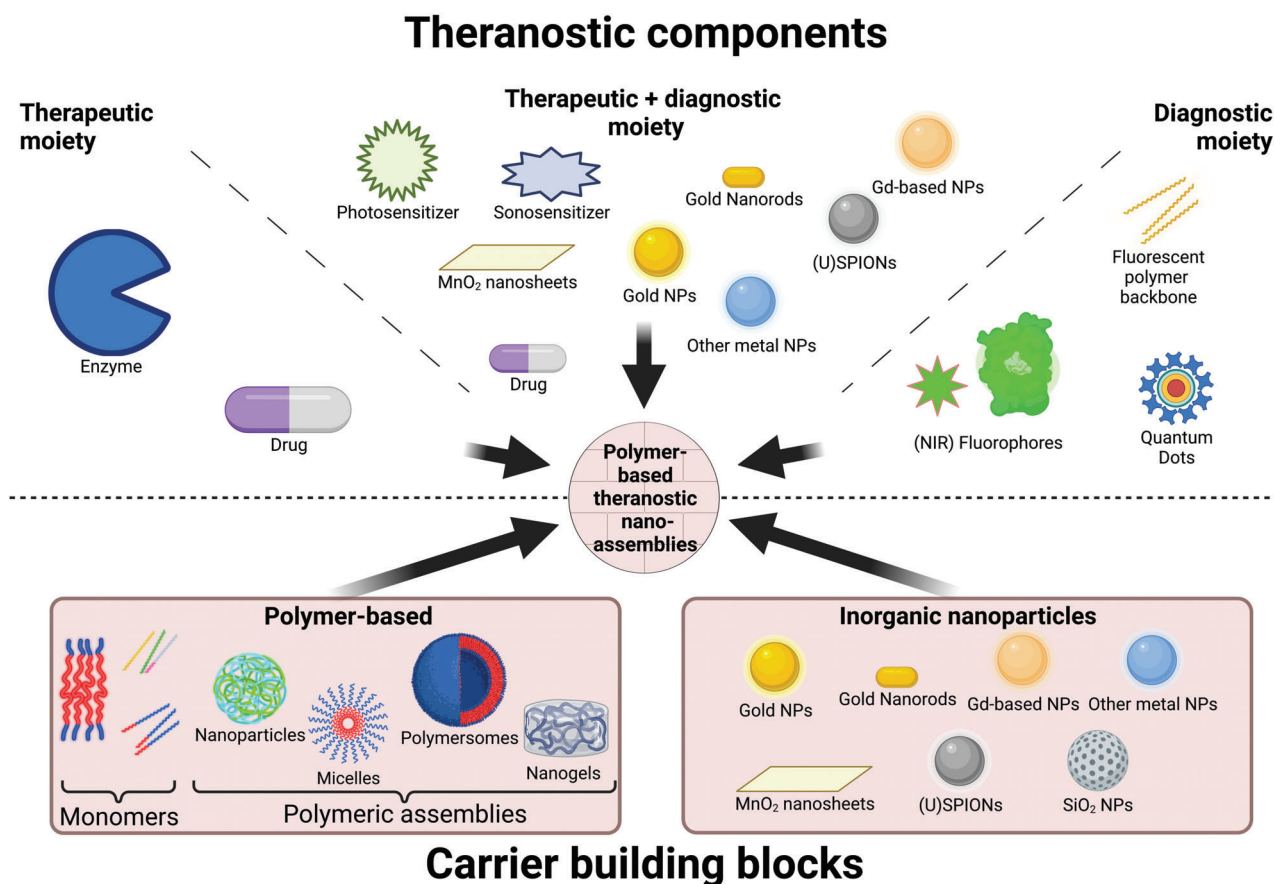
M. S. Muthwill, P. Kong, I. A. Dinu, D. Necula, C. John, C. G. Palivan  
Department of Chemistry  
University of Basel  
Mattenstrasse 24a, BPR 1096, Basel 4058, Switzerland  
E-mail: cornelia.palivan@unibas.ch

M. S. Muthwill, C. G. Palivan  
NCCR-Molecular Systems Engineering  
Mattenstrasse 24a, BPR 1095, Basel 4058, Switzerland

 The ORCID identification number(s) for the author(s) of this article can be found under <https://doi.org/10.1002/mabi.202200270>

© 2022 The Authors. Macromolecular Bioscience published by Wiley-VCH GmbH. This is an open access article under the terms of the Creative Commons Attribution-NonCommercial-NoDerivs License, which permits use and distribution in any medium, provided the original work is properly cited, the use is non-commercial and no modifications or adaptations are made.

DOI: 10.1002/mabi.202200270



**Figure 1.** Polymer-based theranostic nanoassemblies. Theranostic systems composed of two main building blocks, (i) polymers and polymer assemblies, and (ii) platforms containing inorganic nanoparticles. Theranostic components are added to the assembly as combination of therapeutic and diagnostic moieties or as moieties with dual functionality (treatment and diagnostics).

ones of the same size.<sup>[24]</sup> Besides modifying their surface, the functionality of polymer assemblies can be significantly enlarged through the incorporation of inorganic nanoparticles that endow the nanomaterials with multiple therapeutic and/or diagnostic functions.<sup>[15,25–43]</sup>

In addition to physical properties, the design of theranostic systems has to cope with the biorequirements related to therapeutic support with the simultaneous visualization of the region of treatment. Thus, biocompatibility represents an important factor to be considered when developing polymer nanoassemblies for theranostic applications and significant care must be taken to avoid toxicity, mutagenicity, rejection, and inflammatory or immune response. Therefore, the polymer chemistry has to be appropriately selected to provide biocompatible solutions.<sup>[44–46]</sup> Stimuli-responsiveness is another property that allows for precise drug delivery when the conditions in the carrier environment induce a specific change of the carrier architecture/properties promoting the release of the cargo. The stimuli-response can be triggered by various physical or chemical factors, such as temperature, irradiation with a specific wavelength, presence of a magnetic field, pH changes, redox conditions, and the presence of specific biomolecules.

In this review, we present very recent developments in the design and application of theranostic systems based on synthetic

nanoassemblies with a focus on the stimuli-responsive ones. Considering polymer nanoassemblies and inorganic nanoparticles as the main building components, we will mainly present theranostic systems based on i) polymer assemblies, ii) platforms containing inorganic nanoparticles and polymers, and iii) complex architectures combining the polymer assemblies with inorganic nanoparticles (**Figure 1**). We will highlight the chemical nature of copolymers that self-assemble into nano/microsized carriers containing both therapeutic compounds and reporting components for diagnostics. For an efficient theranostic system both the properties of the carriers and the specificity of the biomedical application are essential. The carrier properties and bi-conditions induce crucial limitations requiring a careful selection of polymers, type of assemblies, and manner of administration. One or several therapeutic agents can be loaded inside the supramolecular structure of the assemblies for a combinatorial treatment,<sup>[47]</sup> while contrast agents for imaging are either loaded, chelated, in situ precipitated, or covalently linked to the nanocarrier surface.<sup>[48–52]</sup>

We will present only very few examples of conjugates based on covalent bonding between the polymer/inorganic nanoparticles and the therapeutic and diagnostic compounds, for which there are other excellent reviews.<sup>[53–58]</sup> These systematic surveys mostly report on systems that release the conjugated drug or

reporting molecule as response to one or several stimuli by cleavage of the labile covalent bonds that these moieties have with the self-assembled structure. Here, we focus on the actual development of polymer theranostics with an emerging architecture that mainly relies on self-assembly and entrapment/encapsulation, and whose functionality can be further tailored by incorporation of inorganic nanoparticles. In addition, stimuli-responsiveness represents a key property for reported examples to provide an increased specificity and reduced side-effects, and thus to function as effective sensing and therapeutic systems under pathological conditions.

We will indicate the endogenous and exogenous stimuli triggering the functionality of the theranostic systems, either as a single stimulus or a combination of stimuli. We will emphasize the role of the carriers and how they support the dual functionality required for an efficient theranostic system. An important aspect is the manner in which stimuli-responsive assemblies are designed and applied for theranostics. We are interested to show which systems are responsive to a particular stimulus and which nanoarchitectures are of interest for theranostics. Eventually, we indicate open questions still to be solved or improvements necessary to enhance the efficiency of theranostic systems.

## 2. Endogenous and Exogenous Stimuli Triggering the Response of Theranostic Systems

Implementing stimuli-responsiveness into theranostic systems gives the decisive advantage of controllable and triggerable functions such as the release of cargo. This is an important developmental step toward controlled spatiotemporal behavior of the system, both therapeutically and diagnostically.<sup>[59]</sup> Stimuli-induced response of the system can be caused by one or more stimuli, either endogenous or exogenous, including changes in pH, redox environment, temperature, and the presence of specific biomolecules or an external magnetic field.<sup>[60]</sup> If the therapy relies on drug-delivery, endogenous stimuli-responsiveness is used to induce a morphological response of the supramolecular assembly, such as disassembly into constituents,<sup>[25]</sup> swelling,<sup>[61]</sup> or cleavage of covalent bonds<sup>[25,62,63]</sup> and subsequent decomposition.<sup>[64]</sup> As a consequence of these changes in morphology, the cargo is released. Endogenous stimuli typically used in theranostics are changes in pH, redox state of the surrounding milieu, or the presence of reactive oxygen species (ROS) or biomolecules such as glucose, ATP or enzymes.<sup>[65,66]</sup>

pH change is a widely used stimulus to trigger the response of a theranostic system because different biological environments normally have distinct pH values, or a pH change occurs due to a pathologic condition.<sup>[67]</sup> For anticancer theranostic systems, the acidic microenvironment of tumor tissues is an ideal stimulus.<sup>[68]</sup> Additionally, for organelle-specific targeting, their defined pH is used to trigger the stimuli-responsiveness of the system. Tumors or inflammation sites often provide an acidified environment, which can serve to induce pH-induced swelling, pore formation, disassembly, or degradation of a polymer assembly.

The intracellular redox state is linked to the cell's capability to eliminate ROS and thus react to the presence of redox

pairs, including glutathione (2GSH/GSSG), nicotinamide adenine dinucleotide (phosphate) (NAD(P)<sup>+</sup>/NAD(P)H), and thioredoxin (TrxSS/Trx(SH)<sub>2</sub>).<sup>[69,70]</sup> Another approach is to use the presence of biochemical stimuli. If a suitable "smart" theranostic carrier is designed, selectively induced release of the cargo occurs in the presence of specific molecules present in the environment, serving as biochemical stimuli. These molecules are normally present in high concentrations in an organ, cell, organelle, or under certain pathological conditions. For example, enzymes are very precise stimuli, as they can be very specific for a target site, such as matrix metalloproteinases which are overexpressed in metastatic tumors.<sup>[71]</sup>

Polymer assemblies that are sensitive to exogenous stimuli have the advantage of being remotely controllable from the exterior. Theranostic systems offer traceability *in vivo* by an appropriate imaging moiety, and either once the theranostic assembly has reached its destination, or at a specific time, the drug release can be induced by the external trigger. Temperature is a stimulus that can be used, e.g., in cancer due to the higher energy consumption of the cancer cells. However, it is difficult to predict the temperature in such tissues to fine-tune the physicochemical properties of the theranostic polymeric assemblies accordingly. One popular, indirect approach to produce an increase in temperature is photothermal therapy (PTT). Magnetic-responsive nanotheranostics have been engineered to take advantage of their intrinsic magnetic properties allowing for a better accumulation at the lesion area and facilitating the drug release and tumor ablation by locally generated hyperthermia under an alternating magnetic field (AMF). A less-commonly-used external stimulus is ultrasound. Sonosensitive systems allow for an increased release and enhanced imaging upon ultrasound treatment *in vitro* and *in vivo*.<sup>[72,73]</sup> Photodynamic therapy (PDT) has been considered a promising method in the treatment of various diseases, including malignant and nonmalignant cancers, where ROS are generated by *in situ* activation of photosensitizers to induce apoptosis and/or necrosis of tumor cells.<sup>[74]</sup> As the photosensitizers emit fluorescence upon light excitation, they can be used as contrast agents for tumor near-infrared (NIR) imaging.<sup>[75–77]</sup> Multimodal systems have been obtained by incorporating plasmids, anticancer drugs, and targeting moieties.<sup>[78]</sup>

For the achievement of high-efficiency and -specificity theranostic systems, an important factor is their ability to react to various stimuli, or to hold more than one stimulus as the trigger for a response. Also, the increasing knowledge of disease mechanisms and cellular processes allows for a more precise adaptation to the conditions encountered *in vivo*. The use of polymers and the variety of possible chemical modifications support the development of manifold stimuli-responsive systems. In the following sections, theranostic polymer assemblies responding to endogenous and exogenous stimuli for therapeutic purposes are discussed.

## 3. Polymers and Polymer Assemblies as Building Blocks for Theranostic Systems

There are two different strategies to achieve stimuli-responsive theranostic systems: i) using responsive polymer chains inside the system that will undergo a specific change (e.g., disassembly due to protonation or the change in polymer solubility below or

above the lower or upper critical solution temperature, cleavage of covalent bonds) in the presence of the stimulus, and ii) using nonresponsive polymer chains and combining them with other responsive components (e.g., membrane proteins, enzymes, superparamagnetic iron oxide nanoparticles (SPIONs) or other metal nanoparticles). We present here mainly theranostic systems based on polymers bearing intrinsic stimuli-responsiveness (Table 1). In addition, we will introduce other examples of theranostic systems based on polymers without intrinsic stimulus-responsiveness that have to be combined with responsive moieties to achieve overall responsiveness (Table 2).

### 3.1. Stimuli-Responsive Polymers as Building Blocks for Theranostic Systems

pH-responsive polymers contain either ionizable or acid-cleavable groups.<sup>[86]</sup> Ionizable polymers are protonated or deprotonated, depending on the  $pK_a$  of the functional group and the surrounding pH. The most commonly used anionic polymers (when protonated) contain carboxylic groups, e.g., poly(acrylic acid) (PAA), poly(4-vinylbenzoic acid), poly(aspartic acid) or hyaluronic acid (HA). They may also contain sulfuric acid functional groups such as poly(vinyl sulfonic acid) or boronic acid functional groups, e.g., poly(4-vinylphenylboronic acid). For the inverse reaction, i.e., protonation of cationic polymers, the most commonly used polymers contain an amino function, such as poly(2-dimethylaminoethyl methacrylate) (PDMAEMA), poly(2-diethylaminoethyl methacrylate) (PDEAEMA), poly(lysine) (PLys) or chitosan. Other cationic polymers based on nitrogen-containing groups are poly(4-vinylpyridine), poly(histidine), or polyethylenimine (PEI).<sup>[87]</sup> In this system, PAA is 50% deprotonated at pH 4.5 and deprotonation, i.e., the anionic charge, increases along with the increase of pH, whereas PDMAEMA is 50% protonated at pH 7.5, and protonation, i.e., the cationic charge, increases by decreasing the pH.<sup>[88]</sup> Acid-cleavable polymers normally contain functional groups such as hydrazones,<sup>[62]</sup> acetals or ketals, imines,<sup>[80]</sup> ortho-esters, amides, or silyl derivatives.<sup>[59]</sup> An oxidative environment can trigger cargo release from an assembly based on oxidation-sensitive block copolymers or oxidation-sensitive units. Often sulfide moieties are included in the polymer chains as they are easily oxidized to sulfoxide moieties, inducing a change in the assembly architecture. One example of an oxidation-sensitive polymer is the triblock copolymer poly(ethylene glycol)-*block*-poly(propylene sulfide)-*block*-poly(ethylene glycol), which self-assembles to form vesicular structures that change into micellar, worm-like structures and finally into soluble unimers under oxidative conditions.<sup>[89]</sup> Enzyme-responsiveness was also used as a tool to monitor endocytosis in cancer cells. For example, lysosomal esterases were used to prompt the hydrolysis of polyesters from synthetic L-aspartic acid derivatives.<sup>[63]</sup> Temperature represents a unique stimulus in theranostic applications as it can act either as an endogenous stimulus when infected tissues or tumors have a naturally higher temperature. Temperature can also be an exogenous stimulus with heat applied from an external source. Thermoresponsivity is commonly introduced when the polymers used for designing the theranostic systems have a solubility behavior that changes in response to variations in

temperature. Most often, the thermosensitive nanoassemblies based on NIPAM-containing polymers undergo a reversible phase transition when the temperature of the medium becomes higher than the lower critical solution temperature (LCST).<sup>[90]</sup> As a result, the polymers change from a soluble, hydrated state when the temperature is below the LCST to an insoluble, dehydrated state above the LCST.

### 3.2. Polymer Assemblies as Building Blocks for Theranostic Systems

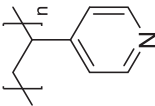
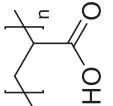
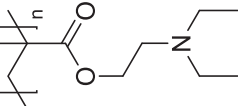
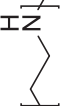
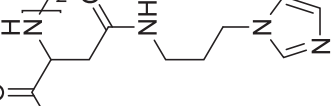
Amphiphilic copolymers undergo self-assembly in dilute solutions to form a variety of nanoassemblies including spherical, cylindrical, gyroidal, and lamellar structures.<sup>[91–93]</sup> In solution, the thermodynamic mismatch causes a phase separation between different blocks and, hence, a morphological reorganization into the above-mentioned shapes in order to minimize the free energy of the system. The resulting architecture depends on various factors, including the hydrophilic to total mass ratio ( $f$  value) of the copolymer, the packing parameter “ $p$ ”, and the dispersity index “ $D$ ” of the copolymer chains.<sup>[91,94,95]</sup>

Spherical nanoassemblies such as nanoparticles, micelles, and polymersomes represent an important class of self-assembled nanostructures that are applied to theranostics. These assemblies are of interest due to their ability to carry multiple compounds based on the intrinsic character of their cargo. In water, lipophilic molecules can be entrapped in the hydrophobic core of the micelle, while the hydrophilic ones can be loaded in the hydrophilic shell. In the case of polymersomes, as hollow spheres, their architecture allows for the encapsulation of hydrophilic molecules in the inner cavity and hydrophobic compounds within the membrane.<sup>[96,97]</sup> There are different methods for the formation of micelles and polymersomes, including film rehydration and solvent exchange<sup>[98,99]</sup> or recently, via flash nanoprecipitation.<sup>[100]</sup>

#### 3.2.1. Nanoparticles

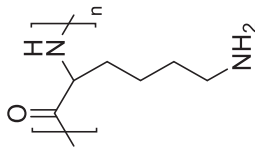
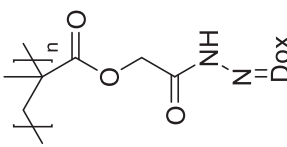
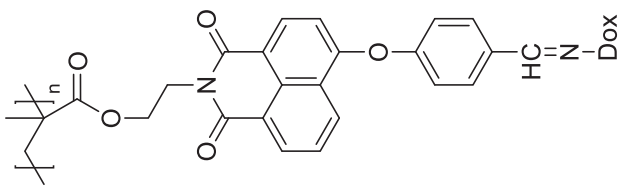
Polymer-based nanoparticles have been extensively investigated in cancer therapeutics as they increase the solubility of poorly soluble drugs, reduce the cytotoxicity toward normal tissues, and improve the treatment efficiency. In addition, imaging agents such as inorganic nanoparticles and organic dyes can also be incorporated via chemical conjugation, electrostatic interaction, or physical encapsulation for simultaneous treatment and imaging.<sup>[101,102]</sup> The accumulation of nanoparticles at the tumor site is commonly improved by conjugation of various targeting moieties such as folate, biotin, peptides, and antibodies on the surface of nanoparticles.<sup>[103,104]</sup> Polymeric NPs are also investigated for theranostic applications in CNS-related and neurodegenerative diseases such as Alzheimer’s and Parkinson’s disease,<sup>[7,8]</sup> in cardiovascular diseases<sup>[11,12]</sup> or visceral leishmaniasis.<sup>[17]</sup> These moieties promote the delivery of therapeutics to a specific site in the body, decreasing their adverse side effects, and facilitate the cellular uptake through receptor-mediated endocytosis. Polymers that can be used in designing polymer nanoparticles for theranostic applications

**Table 1.** Stimuli-responsive polymers used in theranostic systems based on polymeric nanoassemblies, their physicochemical properties as well as additional nonpolymeric moieties.

| Stimulus | Polymer                                  | Abbreviation | Chemical structure   | Hydrophilic/hydrophobic (responsiveness-determining physical parameter) | Assembly type         | Therapeutic moiety/method   | Diagnostic moiety/method                       | Refs. |
|----------|--|--------------|--|---|-----------------------|-----------------------------|--|-------|
| pH       | Poly(4-vinyl pyridine)                   | P4VP         |   | Hydrophilic/hydrophobic ( $pK_a \approx 5.4$ )                          | Core-shell NPs        | DOX/chemotherapy            | AuNRs/PAI, SERS                                | [25]  |
|          | Poly(acrylic acid)                       | PAA          |   | Hydrophilic ( $pK_a \approx 4.5$ )                                      | AuNPs@polymer         | DOX/chemotherapy, AuNPs/PTT | AuNPs/photoacoustic tomography (PAT), X-ray CT | [26]  |
|          | Poly[2-(diethylamino)ethyl methacrylate] | PDEAEMA      |   | Hydrophilic ( $pK_a \approx 7.5$ )                                      | MOF@SH-polymer        | DOX/chemotherapy, Ce6/PDT   | Si-Cd-NPs/MRI, NIR fluorescence                | [27]  |
|          | Poly(ethyleneimine)                      | PEI          |   | Hydrophilic/hydrophobic ( $pK_a \approx 9.7$ )                          | NPs                   | DOX/chemotherapy            | AuNPs/CT imaging                               | [28]  |
|          | Poly( $\beta$ -imidazole-L-aspartate)    | PIA          |  | Hydrophilic ( $pK_a \approx 6.95$ )                                     | Micelles (core-shell) | DOX/chemotherapy, Ce6/PDT   | ESIONS/MRI, fluorescence                       | [29]  |

(Continued)

**Table 1.** (Continued).

| Stimulus | Polymer  | Abbreviation        | Chemical structure   | Hydrophilic/hydrophobic (responsiveness-determining physical parameter) | Assembly type           | Therapeutic moiety/method | Diagnostic moiety/method                | Refs. |
|----------|--|---------------------|--|---|-------------------------|---------------------------|---|-------|
|          | Poly (lysine)  | PLys                |   | Hydrophilic ( $pK_a \approx 10.54$ )                                    | Micelles                | DOX/chemotherapy          | DOX/fluorescence                        | [79]  |
|          | Poly(2-methoxy-2-oxethyl methacrylate-hydrazone-DOX) | PMGMA-hydrazone-DOX |   | Hydrophobic   | Micelles (unimolecular) | DOX/chemotherapy          | DOX/fluorescence                        | [62]  |
|          | Poly (naphthalimide-DOX)                             | PNAP-DOX            |  | Hydrophobic   | NPs                     | DOX/chemotherapy          | Polymer, polymer-DOX/fluorescence, FRET | [80]  |

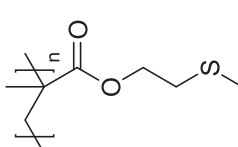

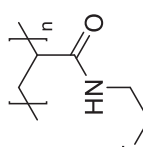
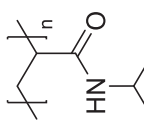
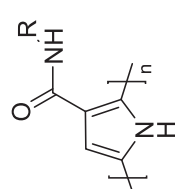
(Continued)

**Table 1.** (Continued).

| Stimulus  | Polymer  | Abbreviation | Chemical structure | Hydrophilic/hydrophobic (responsiveness-determining physical parameter) | Assembly type   | Therapeutic moiety/method                                   | Diagnostic moiety/method   | Refs.   |
|-----------|--|--------------|--------------------|---|---|---|--|---------|
| pH/enzyme | Poly( $\epsilon$ -caprolactone)                                | PCL          |                    | Hydrophobic   | Polymersomes, <sup>[30]</sup> large compound micelles <sup>[31]</sup> | DOX/chemotherapy, <sup>[30]</sup> AuNPs/PTT <sup>[31]</sup> | QDs/MIR, fluorescence <sup>[30]</sup> AuNPs/photothermal imaging, CT <sup>[31]</sup> | [30,31] |
| Redox     | Poly(acrylic acid-SS-DOX)                                      | PAA-SS-DOX   |                    | Hydrophilic   | AuNRs@SH-polymer  | DOX/chemotherapy  | AuNRs/PAI, SERS  | [25]    |
|           | Poly(cystamine methacrylamide)                                 | PCMA         |                    | Hydrophilic   | SiO <sub>2</sub> NPs@polymer  | Au nanowreaths/PTT  | Au nanowreaths/MRI, PAI  | [32]    |
|           | Poly( $\epsilon$ -[2-(ferrocenylcarboxamido)ethyl] acrylamide) | PFCEA        |                    | Hydrophobic (Fc)/hydrophilic (Fc')                                      | Nanogel   | GSK 429286/ $\rho$ kinase inhibition                        | PDFEA (see below), <sup>19</sup> F MRI   | [81]    |

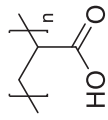
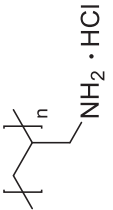
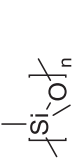

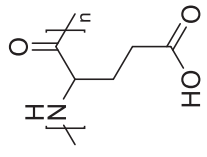
(Continued)

**Table 1. (Continued).**

| Stimulus    | Polymer                                | Abbreviation | Chemical structure  | Hydrophilic/hydrophobic (responsiveness-determining physical parameter) | Assembly type  | Therapeutic moiety/method   | Diagnostic moiety/method  | Refs.         |
|-------------|--|--------------|---|---|--|---|---|---------------|
|             | Poly[2-(methylthio)ethyl methacrylate] | PMTEMA       |    | Hydrophobic   | NPs (core-shell)   | DOX/chemotherapy, Purpurin 18/sonodynamic therapy   | Purpurin 18/PAl, DOX/fluorescence   | [82]          |
| Temperature | Poly( $\epsilon$ -caprolactone)        | PCL          |    | Hydrophobic ( $T_m \approx 60^\circ\text{C}$ )                          | NPs  | IR-780/PDT, paclitaxel/chemotherapy   | IR-780/NIR fluorescence   | [83]          |
|             | Poly[N-(2,2-difluoroethyl)acrylamide]  | PDFEA        |    | Hydrophilic/hydrophobic (LCST $\approx 32\text{--}34^\circ\text{C}$ )   | Nanogel  | GSK 429286/rho kinase inhibition  | PDFEA/ $^{19}\text{F}$ MRI  | [81]          |
|             | Poly(N-isopropylacrylamide)            | PNIPAM       |   | Hydrophilic/hydrophobic (LCST $\approx 32^\circ\text{C}$ )              | Micelles, <sup>[79]</sup> polymeric sponges, <sup>[33]</sup> AuNPs@polymer <sup>[26]</sup> | DOX/chemotherapy, <sup>[26,79]</sup> SPIONs/hyperthermia, <sup>[33]</sup> AuNPs/PTT <sup>[26]</sup> | DOX/fluorescence, <sup>[79]</sup> calcein/fluorescence, <sup>[33]</sup> AuNPs/PAT, CT <sup>[26]</sup> | [26,33,79,84] |
|             | Poly(pyrrole-3-carboxamide)            | PP3CA        |  | Hydrophilic ( $T_g = 44^\circ\text{C}$ )                                | NPs (core-shell)   | DOX/chemotherapy, $\text{Fe}_3\text{O}_4$ NPs/hyperthermia  | $\text{Fe}_3\text{O}_4$ NPs/MRI   | [34,35]       |

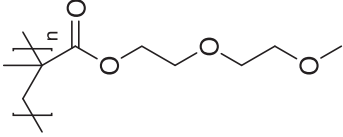
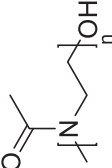
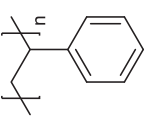



**Table 2.** Summary of theranostics based on polymeric nanoassemblies designed for stimuli-responsiveness located in nonpolymeric moieties.

| Polymer                           | Abbreviation | Chemical structure  | Hydrophilic/<br>hydrophobic | Assembly type   | Stimulus                | Stimulus-responsive moiety   | Therapeutic moiety/method   | Diagnostic moiety/method   | Refs.         |
|-----------------------------------|--------------|---|-----------------------------|---|-------------------------|--|---|--|---------------|
| Poly(acrylic acid)                | PAA          |    | Hydrophilic                 | NR-dimer<br>core-satellite<br>structure                   | Light                   | AuNRs  | Ce6/PDT, AuNRs/PTT  | AuNRs/PAI, MRI<br>(T1-weighted), CT  | [36]          |
| Poly(allylamine<br>hydrochloride) | PAH          |    | Hydrophilic                 | MCO NPs@polymer   | Magnetic field          | SPIONs@PAA   | Cerium oxide NPs/ROS<br>scavenging  | SPIONs/MRI (T2-weighted)   | [15]          |
| Poly(dimethyl siloxane)           | PDMS         |    | Hydrophobic                 | MCO NPs@polymer   | Redox                   | Manganese/cobalt oxide<br>NPs (MCO NPs)  | DOX/chemotherapy  | Mn <sup>2+</sup> , Co <sup>2+</sup> /MRI (T1 and<br>T2-weighted)   | [37]          |
| Poly(ethylene glycol)             | PEG          |    | Hydrophilic                 | MCO NPs@polymer   | Redox                   | MCO NPs  | DOX/chemotherapy  | Mn <sup>2+</sup> , Co <sup>2+</sup> /MRI (T1 and<br>T2-weighted)   | [37]          |
| Poly(L-glutamic acid)             | PGA          |  | Hydrophilic                 | Polymersomes  | Magnetic field          | Enzyme (DDC)   | Dopa carboxylase/enzymatic drug<br>production   | DY-633 polymer-<br>somes/fluorescence<br>colocalization  | [16]          |
|                                   |              |   |                             | Nanoclusters; [38]<br>micelles; [35,40]<br>NPs [34,35,41] | Magnetic field          | SPIONs; [34,35,38,39]<br>superparamagnetic<br>La0.7Sr0.3MnO3<br>nanoparticles NPs<br>(SPMNPs) [41] | Paclitaxel/chemotherapy [38,39]<br>DOX/chemotherapy [34,35,41]<br>SPIONs; [34,35]<br>SPMNPs (41)/hyperthermia,<br>Gd-DTPA/thermal neutron<br>irradiation [40] | SPIONs/MRI [34,35,38]<br>SPIONs/MRI<br>(T2-weighted) [39]<br>SPMNPs/MRI [41]<br>Gd-DTPA/MRI<br>(T1-weighted) [40]<br>Mn <sup>2+</sup> /MRI | [34,35,38–40] |
|                                   |              |   |                             | Nanosheets  | Multiple (pH,<br>Redox) | MnO <sub>2</sub> nanosheets  | DOX/chemotherapy  |  | [42]          |
|                                   |              |   |                             | MCO<br>NPs@polymer [37]<br>micelles [65]                  | Redox                   | MCO NPs [37]<br>DCM-SS-CPT<br>(dicyanomethylene-4H-<br>pyran) [85]                                 | DOX/chemotherapy [37]<br>camptothecin<br>(CPT)/chemotherapy [85]  | Mn <sup>2+</sup> , Co <sup>2+</sup> /MRI (T1 and<br>T2-weighted) [37]<br>DCM/NIR fluorescence [85]   | [37,85]       |
|                                   |              |   |                             | Polymersomes  | Magnetic field          | USPIONs  | DOX/chemotherapy maghemite<br>(γ-Fe <sub>2</sub> O <sub>3</sub> )<br>USPIONs/hyperthermia   | Maghemite (γ-Fe <sub>2</sub> O <sub>3</sub> )<br>USPIONs/MRI   | [43]          |

(Continued)

**Table 2.** (Continued).

| Polymer                                     | Abbreviation         | Chemical structure  | Hydrophilic/<br>hydrophobic | Assembly type                     | Stimulus             | Stimulus-responsive moiety | Therapeutic moiety/method   | Diagnostic moiety/method                                  | Refs. |
|---|----------------------|---|-----------------------------|-----------------------------------|----------------------|----------------------------|---|---|-------|
| Poly[2-(2-methoxyethoxy)ethyl methacrylate] | PMEO <sub>2</sub> MA |    | Hydrophilic                 | Large compound micelles           | Light                | AuNPs                      | AuNPs/PTT   | AuNPs/photothermal imaging, CT                            | [31]  |
| Poly(2-methyl-2-oxazoline)                  | PMOXA                |    | Hydrophilic                 | Polymersomes                      | Biomolecule (L-DOPA) | Enzyme (DDC)               | Dopa carboxylase/enzymatic drug production  | DY-633 polymer-somes/fluorescence colocalization          | [16]  |
| Poly(styrene)                               | PS                   |   | Hydrophobic                 | NR-dimer core-satellite structure | Light                | AuNRS                      | Ce6/PDT   | AuNRS/PAI, MRI (T1-weighted), CT                          | [36]  |
| Poly(trimethylene carbonate)                | PTMC                 |  | Hydrophobic                 | Polymersomes                      | Magnetic field       | USPIONS                    | DOX/chemotherapy maghemite (γ-Fe <sub>2</sub> O <sub>3</sub> ) USPIONS/hyperthermia | Maghemite (γ-Fe <sub>2</sub> O <sub>3</sub> ) USPIONS/MRI | [43]  |

should include either biodegradable synthetic polyesters (e.g., poly( $\epsilon$ -caprolactone), polylactide, polyglycolide), polycarbonates, polyamides, and polypeptides, among others, or polysaccharides such as chitosan, dextran, heparin, and hyaluronic acid. Recently, polynorbornene copolymers have also been proposed for designing tailor-made stimuli-responsive nanoparticles for multiplexed detection and drug release by anchoring MRI contrast agents, anticancer drugs and active targeting moieties to the same polymer backbone.<sup>[48,49]</sup>

### 3.2.2. Micelles

Polymeric micelles with sizes between 10 and 100 nm in diameter are optimal for long-term blood circulation, since particles smaller than 5 nm are likely to be cleared by the kidneys and particles larger than 100 nm by the liver.<sup>[105]</sup> However, bigger micelles up to 200 nm in diameter, depending on the respective block lengths, have also been reported for delivery of various cargos.<sup>[79,63]</sup> There are two ways to incorporate cargo inside micelles: physical entrapment and covalent conjugation. To increase selective accumulation at the target site, e.g., a tumor<sup>[85]</sup> or in the lungs<sup>[14]</sup> and to avoid severe side effects through non-specific cargo release, the micelles are usually conjugated with a recognition compound and possess a stimuli-responsive feature specific to the targeting medium, such as environmental pH or glutathione (GSH) concentration.<sup>[106]</sup>

One of the most commonly hydrophilic blocks in amphiphilic copolymers is PEG because it allows for the conjugation of diverse active drugs or biomolecules and forms a protective shell to prolong the life span of active compounds.<sup>[107]</sup> Despite the ongoing scientific discussion about side-effects of PEG such as allergic reactions and anaphylactic shock,<sup>[108–112]</sup> PEG-containing amphiphilic block copolymers are extensively used and have been reported for micelle- or polymersome-based theranostic systems.<sup>[113]</sup>

### 3.2.3. Polymersomes

Polymersomes, with their hollow spherical architecture, either have a unilamellar membrane, when amphiphilic triblock copolymers are self-assembled, or a bilayer membrane when amphiphilic diblock copolymers or grafted amphiphilic polymers are used.<sup>[114]</sup> To ensure an efficient cargo release, one common approach is to add a responsive moiety to trigger their dissociation through endogenous stimuli such as pH, redox-based environment, or temperature change.<sup>[115]</sup> Due to their architecture, which allows for the encapsulation of hydrophilic molecules in their cavity and insertion of hydrophobic ones in the membrane, polymersomes are widely reported as carriers or building blocks for theranostic systems.<sup>[52,116]</sup> Depending on the chemical nature of the polymer chains, polymersomes can have intrinsic stimuli-responsiveness, thus changing their architecture upon the presence of the stimulus.<sup>[30,33,116]</sup> A complementary approach forms polymersomes from nonresponsive polymer chains and renders them stimuli-responsive by the insertion of biopores or membrane proteins in the polymer membrane. These biopores/membrane proteins serve as responsive “gates” opening

in the presence of the stimulus and supporting the release of the cargo or the product of an in situ reaction.<sup>[117,118]</sup>

## 4. Inorganic Nanoparticles as Building Blocks for Theranostic Systems

We will first present theranostic systems containing inorganic nanoparticles because here we have examples that have received approval from the United States Food and Drug Administration or European Medicines Agency for their use in nanomedicine.<sup>[119,120]</sup> The preparation methods of inorganic nanoparticles are based on either bottom-up or top-down approaches.<sup>[121,122]</sup> To achieve self-assemblies of inorganic nanoparticles, surface modification is necessary to obtain the amphiphilicity required for the self-assembly process into complex architectures. The surface of unmodified inorganic nanoparticles is functionalized with exposed hydroxyl groups that can further be modified by various treatments, such as polymer grafting and ligand exchange.<sup>[123]</sup> Another approach is the coordination of metals with polyphenols, which have excellent biocompatibility and easily self-assemble to form nanoparticles.<sup>[124]</sup>

Gold NPs are widely used in different theranostic applications due to their chemical and physical versatility. While intrinsically, gold NPs are well suited to imaging (either by irradiation with a laser for PTT)<sup>[26,31,32]</sup> or as a computed tomography (CT) contrast agent,<sup>[14]</sup> they can be surface-functionalized with different therapeutic molecules and polymers to combine therapy and diagnosis.<sup>[31]</sup>

Iron-oxide-based NPs, such as SPIONs, support another type of diagnosis and therapy combination because they generate heat under alternating magnetic fields and, hence, cause tumor cell death,<sup>[33–35]</sup> or they are preferentially up-taken by macrophages to monitor atherosclerotic plaques in cardiovascular diseases.<sup>[72]</sup>

Gadolinium NPs are widely used contrast agents for magnetic resonance imaging (MRI),<sup>[97]</sup> therefore they are often included in theranostic assemblies as well. In a different approach, magnetic NPs are of interest due to their dual capability for diagnosis using MRI and for treatment using hyperthermia. Magnetic-responsive theranostics architecture rely on iron oxide NPs, iron oxide hybrid NPs (with Au, Ag, Gd), or other magnetic materials (e.g.,  $\text{ZnFe}_2\text{O}_4$ ,  $\text{La}_{0.7}\text{Sr}_{0.3}\text{MnO}_3$ ).

## 5. Methods for Characterization of the Building Blocks of Theranostic Systems

A combination of physical and chemical methods is used for the characterization of nanoassemblies, including transmission and scanning electron microscopy (TEM and SEM, respectively), light scattering techniques, and nanoparticle tracking analysis. In addition, the morphology of the nanoparticles is investigated by atomic force microscopy, while their composition can be determined by elemental analysis.<sup>[125]</sup> When the theranostic assemblies contain metal-based NPs, they can be characterized by Ferromagnetic Resonance and Superconducting Quantum Interference Device Magnetization measurements.<sup>[126]</sup> Normally, the drugs loaded inside the theranostic systems are spectroscopically characterized and the method of choice depends on their intrinsic chemical nature.

## 6. Combination of Inorganic Nanoparticles and Polymers for Theranostic Systems

There is a variety of combinations with inorganic materials that can be used as platforms in theranostic applications. There are different approaches to develop theranostic systems containing inorganic nanoparticles. Core-shell nanoparticles can contain inorganic metallic NPs at their core, while their surface is usually grafted or covered with a polymer matrix in which a therapeutic compound is either covalently bound or encapsulated. Another method is the encapsulation of NPs into a stimuli-responsive polymer matrix in order to allow their release when the target is reached. Besides classical cancer theranostics, polymer-coated inorganic nanoparticles, either intrinsically bearing theranostic properties, or only diagnostic ones and being additionally loaded with specific therapeutics, are also investigated in cardiovascular diseases<sup>[11]</sup> or genetic diseases.<sup>[13]</sup>

### 6.1. Single Stimulus-Responsiveness of Inorganic Nanoparticles Combined with Polymers

We present relevant examples based on inorganic nanoparticles and polymers that form assemblies for theranostic purposes. Extremely small iron oxide nanoparticles (ESIONs) of less than 4 nm were coated with amphiphilic and pH-responsive block copolymers to generate colloidal magneto-core-shell structures, named “pH-sensitive magnetic nanogrenades” (PMNs).<sup>[29]</sup> The poly(ethylene glycol)-*block*-poly( $\beta$ -benzyl-L-aspartate) block copolymers were end-functionalized by a chlorin e6 (Ce6) photosensitizer, (PEG-PBLA-Ce6), and modified either with 1-(3-aminopropyl) imidazole (API) and dopamine or with API and 3-phenyl-1-propylamine. The ESION-polymer coassembly was induced by solvent exchange from chloroform to the more polar dimethyl sulfoxide. PMNs with a size of  $70 \pm 5$  nm were formed and deemed adequate for passive tumor targeting. The ligands were designed for two-stage pH activation: i) the decrease of pH in tumoral medium induced the swelling of PMNs and delivery of their payload, and ii) in the endosomal pH 5.5–6.0, dissociation of the nanotheranostics induced an enhancement in  $T_1$  MR imaging, fluorescence, and photodynamic therapeutic activity.<sup>[29]</sup>

In a more complex architecture, AuNPs serving for CT imaging were embedded into a hybrid system based on laponite (LAP) nanodisks assembled with PEI conjugated with poly(lactic acid)-*block*-poly(ethylene glycol) (PLA-*b*-PEG-COOH). LAP-PLA-*b*-PEG-PEI was modified with HA and Doxorubicin (DOX) to actively target the CD4 receptors overexpressed in tumor cells. The developed LAP-PLA-*b*-PEG-PEI-(Au<sup>0</sup>)<sub>50</sub>-HA/DOX showed good stability, high drug loading capabilities, and pH-sensitive drug release.<sup>[28]</sup>

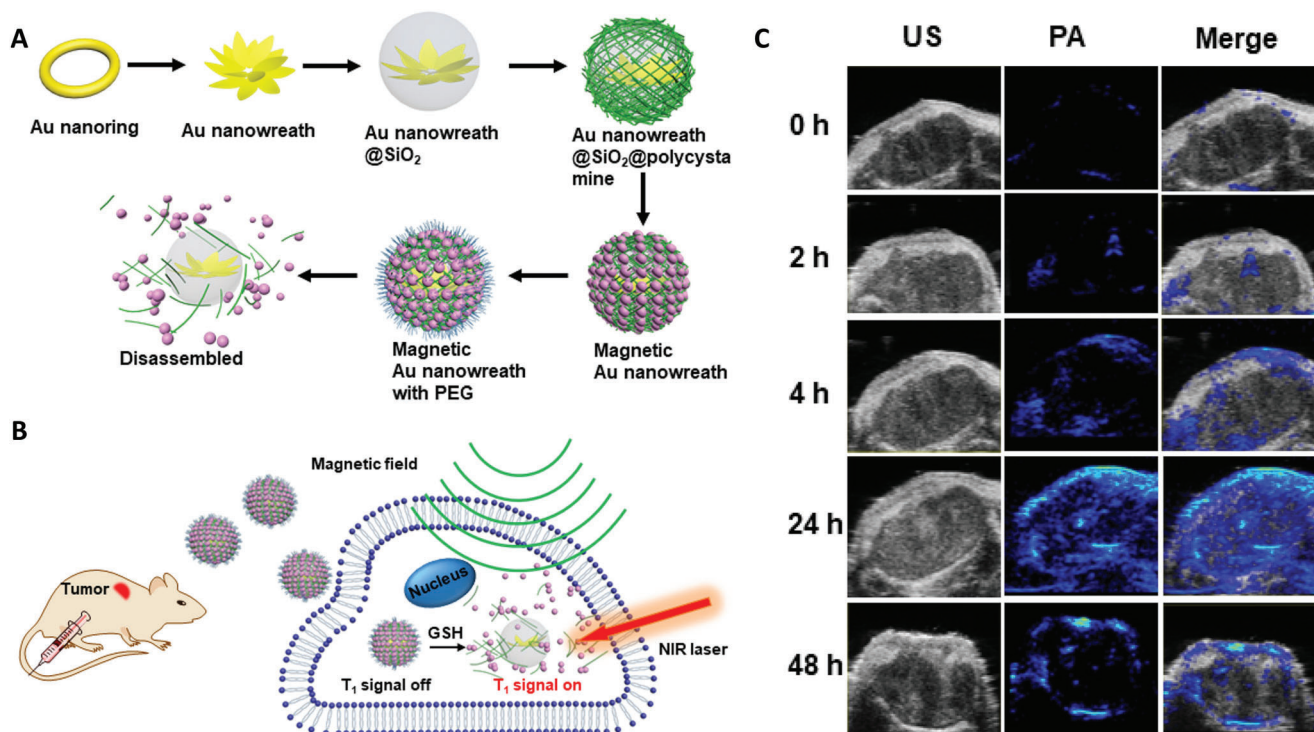
An interesting approach to include AuNPs in more complex architectures was achieved by synthesis of Au nanowreaths (AuNWs) from seed-mediated growth of Au nanorings followed by a coating with thiol-terminated PEG. The resulting AuNWs served further as support for the formation of larger assemblies using the consecutive layer-by-layer (LbL) deposition of positively charged copolymer poly[cystamine methacrylamide-*co*-poly(ethylene glycol) methyl ether methacrylate] and negatively charged small magnetic iron oxide nanoparticles (ES-MIONs).

As the AuNWs absorb in the NIR domain, they allow for the photoacoustic imaging (PAI) and photoablation of the tumor. The resulting LbL assemblies provided a better MRI contrast than ES-MIONs alone. Together, the assembled ES-MIONs on AuNWs quenched the  $T_1$ -weighted MRI signal due to enhanced  $T_2$ -weighted decay while the nanoplatform disassembled in the presence of GSH found in high concentration in tumor cells by disulfide bond cleavage. The destabilization of the LbL assembly switched the  $T_1$  signal on and thus enhanced the image contrast (Figure 2).<sup>[32]</sup>

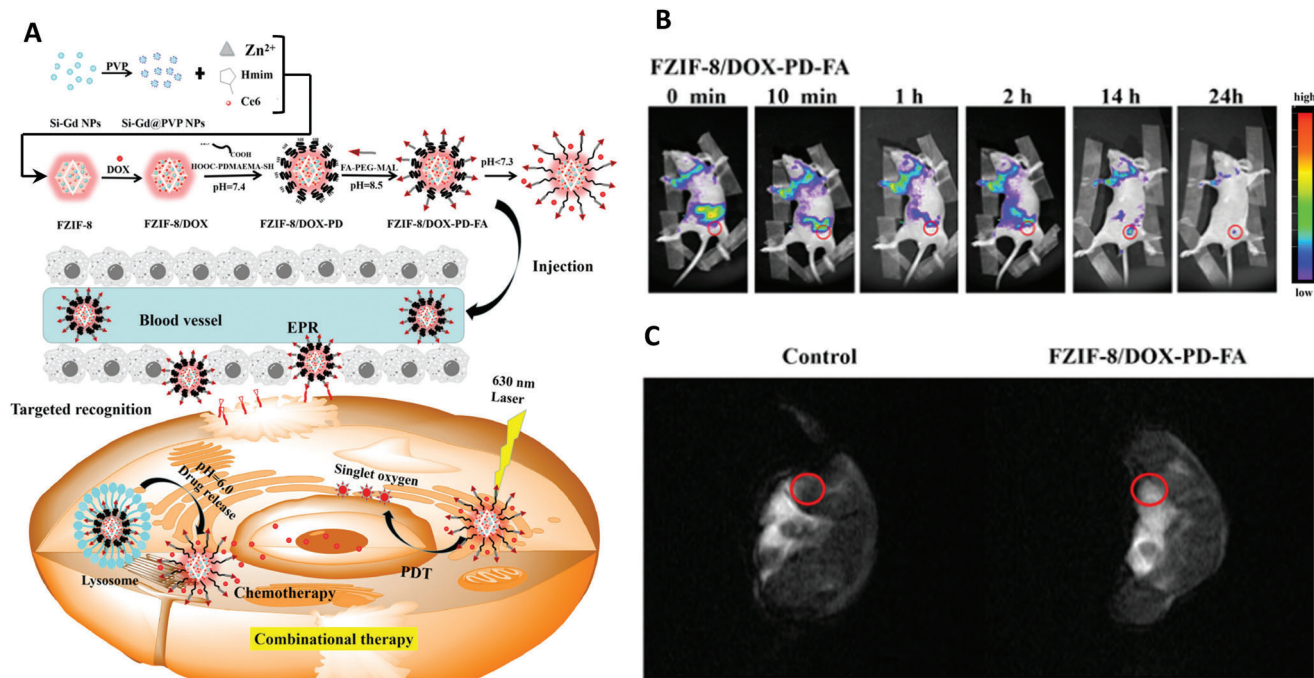
Gd-doped silicon NPs (Si-Gd NPs) were used for self-assembly with a complex metal-organic framework (MOF), resulting in a pH-responsive cancer theranostic system with dual diagnostic capability (MIR and NIR fluorescence) and dual therapeutic function (chemotherapy and PDT) (Figure 3). The pH-responsive poly[2-(diethylamino)ethyl methacrylate] (HOOC-PDMAEMA-SH) polymer was grafted together with folic acid-poly(ethylene glycol)-maleimide (MaL-PEG-FA) to a zeolitic imidazolate framework-8 (ZIF-8) that served as a biocompatible and biodegradable nanocarrier. Si-Gd NPs and a photosensitizer (Ce6) were coembedded into ZIF-8, and then loaded with DOX.<sup>[27]</sup> This complex MOF served in vitro and in vivo for drug release at pH 6 through the swelling of the pH-responsive polymer, PDT by irradiation of Ce6 with NIR, and dual modal imaging by MRI and fluorescence (Si-Gd-NPs).

Ag<sub>2</sub>S nanodots (Ag<sub>2</sub>S NDs) were rendered pH-responsive by self-assembly with poly(ethylene glycol)<sub>5k</sub>-*block*-poly( $\beta$ -aminoesters)<sub>10k</sub> (PEG<sub>5k</sub>-*b*-PAE<sub>10k</sub>) and loaded with Hsp70 inhibitor to reduce the thermoresistance often found in cancer cells due to the upregulation of heat-shock proteins. Ag<sub>2</sub>S NDs allow for PAI-guided PTT and the pH-responsiveness led to the enhanced release of inhibitor molecules. The assembly showed good biocompatibility and preference for accumulation in lysosomes. Additionally, PAI allows for the tracing of therapeutic agents and the individual length of therapy time.<sup>[127]</sup> In another approach, gold nanorods (AuNRs) were used for conjugation with a mixture of light-responsive prodrug of ruthenium-complex (PolyRu) and PEG, resulting in a theranostic system AuNR@PEG/PolyRu. PolyRu was obtained by coordination of the Ru-complex [Ru(tpy)(biq)](PF<sub>6</sub>)<sub>2</sub> with the cyan group from poly[6-(4-cyanophenoxy) hexyl methacrylate]. The self-assembly was achieved by the microemulsion technique in the presence of an NIR-II fluorescence dye (IR1061). Therefore, in vivo, when the theranostic system was NIR-irradiated, it disassembled and released the Ru-complex that acted as a chemotherapy drug and a photodynamic therapy for cancer, as well as IR1061, which was quenched by AuNRs but recovered its fluorescence.<sup>[128]</sup>

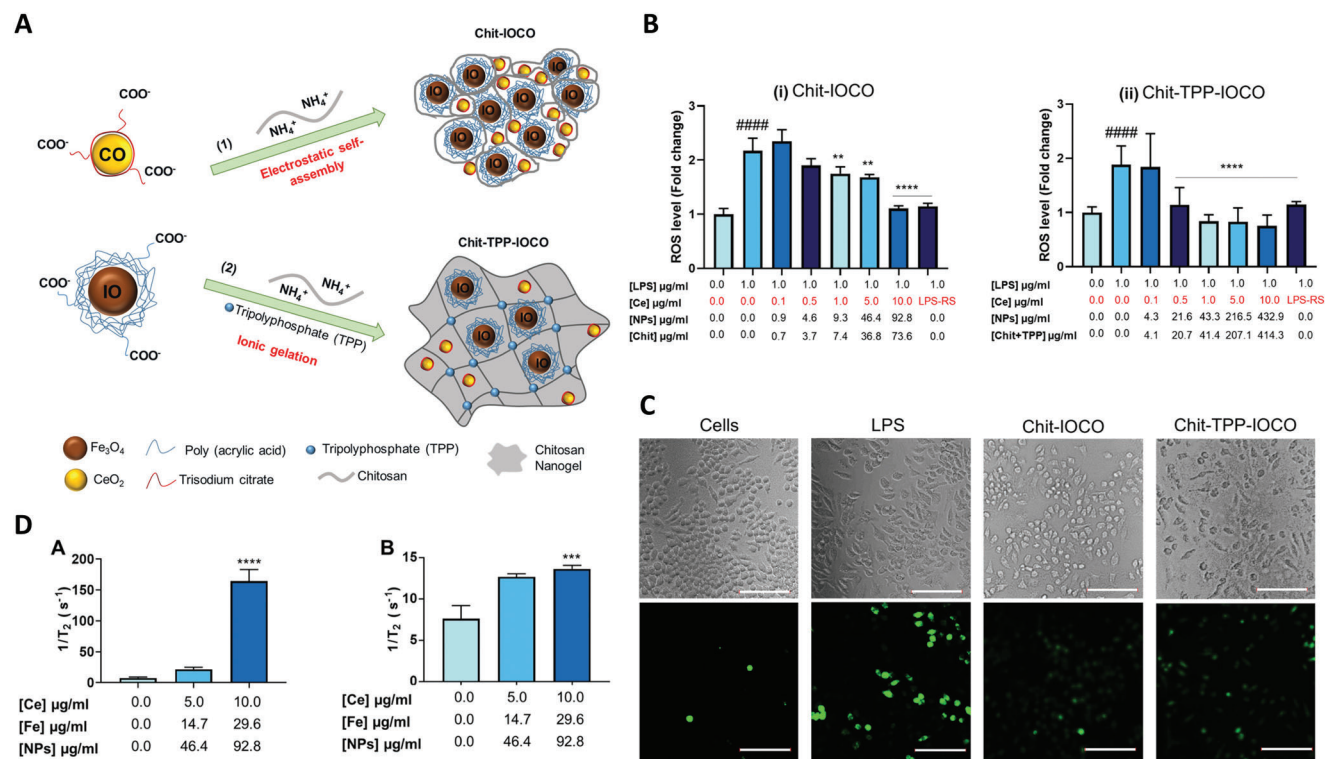
Magnetic nanotheranostics have largely been used for theranostic systems because they rely on AMF-induced hyperthermia for the drug release, but also to help overcome drug resistant cancers when the drug and hyperthermia are used synergistically. A prime example of the synergetic effect in cancer treatment by magnetic nanocarriers is based on superparamagnetic La<sub>0.7</sub> Sr<sub>0.3</sub> MnO<sub>3</sub> nanoparticles (SPMNPs) functionalized with oleic acid-poly(ethylene glycol) and loaded with DOX by carbodiimide coupling chemistry.<sup>[41]</sup> The system was efficient; in 30 min in vitro tests conducted under AMF, induced hyperthermia showed cancer cells death rates to levels similar to those observed in free-DOX experiments after 24 h. In the absence of



**Figure 2.** A) Preparation of Au nanowreaths (AuNWs). B) In vivo GSH-responsive disassembly and application of PAI by NIR irradiation and enhanced T1-weighted MRI ES-MIONS. C) Ultrasonic (US) and photoacoustic (PA) and merged images of tumor in mice after AuNWs injection. Reproduced with permission.<sup>[32]</sup> Copyright 2018, American Chemical Society.



**Figure 3.** A) Synthesis of theranostic, pH-responsive, and active-targeting metal–organic frameworks (MOFs) nanocarriers for combined chemotherapy and PDT together with NIR FI. B) In vivo NIR FI of tumor in mice after intraperitoneal injection of MOFs. C) In vivo MR images of tumor-bearing mouse after treatment with theranostic MOFs with tumor sites labeled, showing a strong signal at tumor site. Reproduced with permission.<sup>[27]</sup> Copyright 2019, American Chemical Society.



**Figure 4.** A) Preparation of ROS-scavenging chitosan NPs containing  $\text{Fe}_3\text{O}_4$  (IO) and  $\text{CeO}_2$  (CO) by either electrostatic self-assembly or ionic gelation. B) ROS scavenging ability of Chit-IOCO and Chit-TPP-IOCO nanoparticles in macrophages treated with different nanoparticles at different concentrations. Significant reduction reached at a  $\text{CeO}_2$  concentration of  $1 \mu\text{g mL}^{-1}$  (i) and  $0.5 \mu\text{g mL}^{-1}$  (ii). C) ROS levels in treated cells measured by fluorescence imaging (green signal), showing the ROS-scavenging effect of Chit-IOCO and Chit-TPP-IOCO nanoparticles. D) In vitro T2-weighted MRI signal of macrophages treated with Chit-IOCO and Chit-TPP-IOCO nanoparticles in dependency of  $\text{Fe}_3\text{O}_4$  concentration. Reproduced (with permission,<sup>[15]</sup> Copyright 2021, American Chemical Society.

the magnetic field, the theranostic system behaved no differently from the free-DOX tests, underlining the importance of the synergistic effect.

In another example, magnetite ( $\text{Fe}_3\text{O}_4$ ), with its low toxicity, low price, and high magnetization served for the development of magnetic-responsive polymeric smart-nanoparticles ( $\text{Fe}_3\text{O}_4/\text{DOX}/\text{PPy}/\text{PEG}/\text{FA}$  NPs) whose poly(pyrrole-3-carboxylic acid) (PPy) core was loaded with DOX. The latter was released through softening of the polymer phase, which displays a glass transition temperature ( $T_g$ ) of  $44^\circ\text{C}$ .<sup>[34]</sup> The combination of magnetic hyperthermia and chemotherapy resulted in the successful treatment of multiple myeloma, without tumor recurrence. The system was further developed, bringing forward new biocompatible smart nanoparticles<sup>[35]</sup> with a tightly clustered magnetite core that improved the relaxivity and the heat-generation power. This theranostics system allowed for a constant stream of highly targeted chemotherapeutics for days or even weeks, as the drug release continued even after removing the magnetic field.

Chitosan-based nanoassemblies as carriers for both PAA-coated iron oxide (IO-PAA) NPs and trisodium citrate coated cerium oxide NPs were developed to treat ROS-related diseases, including atherosclerosis and rheumatoid arthritis. The self-assemblies were produced by electrostatic interaction between positively charged chitosan and negatively charged (IO-PAA) NPs. Iron oxide nanoparticles allowed for the detection of ROS, while cerium oxide or nanoceria served as ROS-scavengers.

These nanoassemblies showed an excellent anti-ROS efficiency and MRI contrast, making them potential theranostic agents in simultaneous treatment and diagnosis of ROS-related diseases (Figure 4).<sup>[15]</sup>

## 6.2. Dual Stimuli-Responsiveness of Inorganic Nanoparticles Combined with Polymers

AuNRs were used for a core-shell assembly with dual pH- and redox-responsiveness. The theranostic system with a size of  $\approx 70$  nm was generated through covalent attachment of DOX to the AuNRs via a cleavable disulfide bond ( $\text{AuNR}@\text{PDOX}$ ) and subsequent encapsulation into a core assembled from the pH-responsive amphiphilic diblock copolymer poly(ethylene glycol)-*b*-poly[(2,5-bis[(4-carboxylicpiperidylamino)thiophenyl]croconine)-*co*-(4-vinyl pyridine)] (PEG-PCRVP).<sup>[25]</sup> The core-shell assembly  $\text{PEG-PCRVP}/\text{AuNR}@\text{PDOX}$  was able to disassemble the pH-responsive polymeric shell at low pH, which facilitated the disassociation of  $\text{AuNR}@\text{PDOX}$  clusters into single AuNRs@PDOX nanoparticles, more easily penetrating the tumor. Due to the high concentration of GSH located in the tumor cells, the disulfide bond was cleaved and hence DOX was released while AuNRs allowed for enhanced deep-tissue PAI and, thanks to plasmonic coupling of AuNRs, surface-enhanced Raman scattering<sup>[129]</sup> in real-time for in vivo studies and therapy.

In melanoma cells (MDA-MB-435), the hybrid nanoparticles showed a high, concentration-dependent cytotoxicity of  $\approx 80\%$  at the highest concentration, which could be increased upon laser irradiation, activating PTT. In addition, treatment of melanoma tumors in vivo with this theranostic system and additional laser treatment inhibited the tumor growth by 96.5%.<sup>[25]</sup>

pH and temperature dual responsiveness is desirable because in cancerous tissues, not only is the pH abnormal, but the temperature is as well. This dual responsiveness was achieved with polymer@AuNPs loaded with DOX.<sup>[26]</sup> The combination of stimuli-responsive polymer with AuNPs enabled a therapeutic, chemo-photothermal approach. A biocompatible and dual responsive triblock copolymer, HS-PCL-*b*-PNIPAM-*b*-PAA, was grafted on gold NPs via a covalent Au-S bond. DOX was loaded on the polymer through hydrogen bonding between PAA and DOX at physiological pH. Upon a pH drop, the H bonds are cleaved, leading to increased drug release. Hence, PAA imparts the polymer with pH-responsiveness. The thermoresponsiveness is originating from PNIPAM, whose LCST can be tuned to 43–45 °C when copolymerized with hydrophilic blocks. Phase transition with increasing temperature then leads to a structural change of the PNIPAM block. It was demonstrated in vitro that the DOX release was increased upon both pH decrease from 7.4 to pH 4.0 and temperature increase from 37 to 46 °C. In vitro cytotoxicity showed good biocompatibility of the NPs and a high concentration-dependent, chemotherapeutic potential of the drug-loaded particles in breast cancer cells (MCF7) which was enhanced compared to the free drug. Combination with phototherapy by irradiation with a pulsed laser at 1064 nm led to high cytotoxicity of DOX-loaded polymer@AuNPs. However, the study lacks a control in the form of untreated cells, which are essential for the evaluation of the cytotoxic effect on tumor cells. Also, no in vivo experiments were conducted. The particles were not equipped with targeting moieties; hence, the effect only relies on passive targeting.

Manganese oxide (MnO<sub>2</sub>) served to develop nanosheets that have been combined with anticancer drugs, the resulting assembly served to treat and diagnose tumors. MnO<sub>2</sub> nanosheets with a size of 20–60 nm were amine-functionalized at their surface by reacting with (3-aminopropyl)trimethoxysilane, and then PEGylated with hetero-functionalized PEG (NH<sub>2</sub>-PEG-COOH). Then, DOX was loaded through adsorption on the nanosheets surface, while folic acid was conjugated to efficiently target the tumor cells. MnO<sub>2</sub>-PEG-FA/DOX assembly was able to disintegrate in the slightly acidic medium and high concentration of GSH that is specific to cancer cells. These dual redox and pH-responsive biodegradable nanosheets disintegrated into manganese ions serving as contrast agents for MRI, while DOX supported efficient cancer treatment.<sup>[42]</sup> Based on the same concept, hollow spheres of an alloy of manganese/cobalt oxide (MCO) with a size of 70 nm were loaded with DOX by diffusion and electrostatic interaction. Upon disintegration under a slight change in pH and the presence of GSH in tumor cell, the anticancer drug was released while the manganese ions improved the contrast for MRI.<sup>[37,130]</sup>

A theranostic platform was developed by complexing metal ions (Gd<sup>3+</sup>, Fe<sup>3+</sup>, Mn<sup>2+</sup>) as MRI contrast agents with dicycysteine copolymerized with DOX (poly(dicycysteine-*co*-TEP-*co*-DOX)). The assembly served as a pH- and redox-responsive

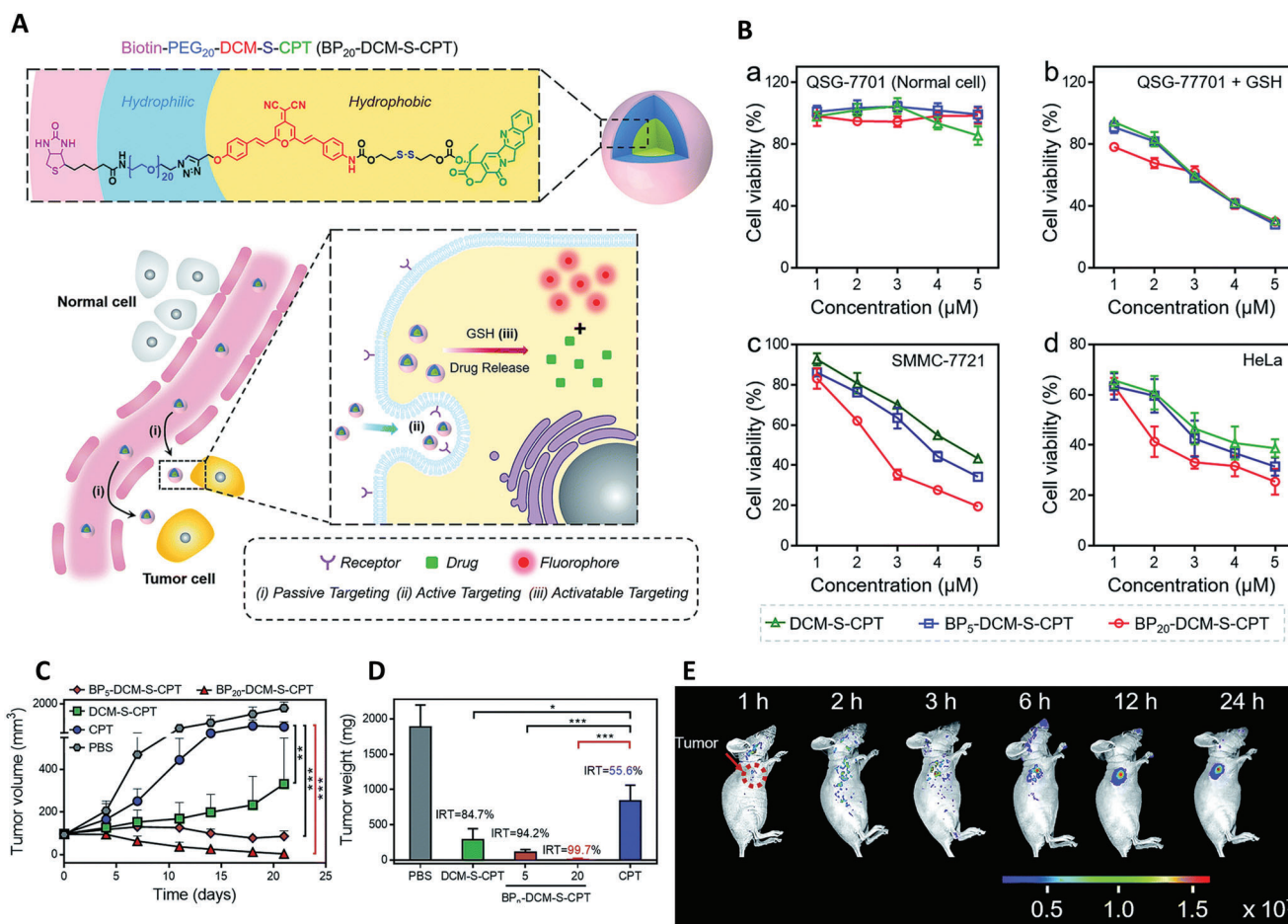
polyprodrug and contrast agent. Both stimuli lead to the degradation of the nanoassemblies and release of the drug and contrast agents in vitro and in vivo.<sup>[131]</sup> A controllable self-assembly of gold NPs grafted with a mixture of thiol-functionalized poly( $\epsilon$ -caprolactone) (PCL) and poly[2-(2-methoxyethoxy) ethyl methacrylate] (PMEO<sub>2</sub>MA) has been reported as a promising treatment for human breast cancer using PTT. The polymer-coated AuNPs self-assembled into vesicles or large compound micelles that allowed the reduction of the distance between NPs and induced a red-shift in the NIR region, which is suitable for PTT. Addition of esterase for the hydrolysis of PCL ester bonds and the generated heat provoked the disassembly of the micelles, and AuNPs served to monitor the region by photothermal imaging or in vivo imaging by X-ray CT.<sup>[31]</sup>

## 7. Polymer Assemblies as Theranostic Systems

### 7.1. Single Stimulus-Responsiveness of Polymer Nanoassemblies

An interesting and simple theranostic approach also exploiting DOX fluorescence was realized by a pH-sensitive polymer-prodrug system favoring intramolecular fluorescence resonance energy transfer (FRET).<sup>[80]</sup> Coupling the fluorescent polymer (FRET donor) covalently with the fluorescent DOX (FRET acceptor) via acid-labile imine bond allows for FRET-based tumor tracking and site-selective drug release. The polymer-prodrug self-assembled into nanoparticles with a diameter of 71 nm and narrow size distribution. Upon internalization by endocytosis, the low pH in endosomes and lysosomes lead to the cleavage of polymer-prodrug and reversal of FRET, causing a shift in the fluorescence emission from orange to blue. Additionally, DOX can be monitored by its own fluorescence. This approach allows for self-tracking of pH response and drug release as well as to reduce the toxic side-effects of DOX by increasing the specificity via polymer-prodrug stability. Triggered drug-release by acidic pH was observed (more than 90% release at pH 5 after 129 h compared to 6.3% at pH 7.4). There was no toxicity of control polymer particles on HepG2 cells after 24 h, but no data is given for 48 and 72 h. DOX killed cells more efficiently after 24 h when applied via the nanoparticles, but after 72 h there was no observed difference from free DOX. FRET reversal and thus drug release were confirmed in solution and in vitro (HepG2) by internalization into nuclei. While this simple approach combines site-specificity with stimulus-responsiveness and live-monitoring of drug release, there are still steps to be undertaken to transfer such systems to in vivo application.

By using thermosensitive PCL, nanoparticles stabilized with albumin in combination with an entrapped photosensitizer, it was possible to develop an efficient system for PDT.<sup>[83]</sup> The system, designed for the treatment of drug-resistant tumors, combines an NIR fluorescent dye (IR-780) as a photosensitizer for PDT with paclitaxel, a chemotherapeutic drug. Excitation of the dye produced heat and generated ROS. PCL, which has a low melting temperature of around 60 °C, showed increased drug release upon heating. Additional surface modification of the nanoparticles with a peptide specific to the luteinizing hormone-releasing receptor allowed for active targeting of the system. A high drug-loading capacity and encapsulation efficiency, as well as selective accumulation in ovarian cancer cells in a mouse



**Figure 5.** A) Theranostic active-cancer cell targeting micelles with GSH-responsiveness self-assembled from amphiphilic diblock-copolymer containing biotin for active targeting, an NIR fluorescence imaging moiety (DCM) as well as a chemotherapeutic drug (CPT) covalently bound to the polymer as a prodrug via redox-cleavable disulfide bond. Upon passively targeting the tumor tissue (EPR effect), receptor-mediated endocytosis due to active biotin receptor targeting, the micelles are internalized and respond to high GSH concentration by prodrug cleavage and drug release. In vivo NIR fluorescence imaging allows for tracking the theranostic assemblies. B) In vitro cytotoxicity studies (MTT assay) of concentration-dependent effect of micelles of different polymer composition with three cell lines: (a) human hepatocyte QSG-7701 cells, (b) QSG-7701 cells + 2.5 mM GSH, (c) human hepatoma SMMC-7721 cancer cells, and (d) HeLa cancer cells. C) In vivo anticancer activity shown by tumor volume in tumor-bearing mice after intravenous injection of theranostic micelles and control (PBS) (10 mg kg<sup>-1</sup> every 3 days). D) Mean tumor weight after separation from mice (see C). Inhibition rates of tumor growth (IRT) were calculated as follows: IRT (%) = 100 × (mean tumor weight of control group – mean tumor weight of experimental group)/mean tumor weight of control group. E) In vivo NIR-fluorescence imaging after intravenous injection of BP<sub>20</sub>-DCM-S-CPT into tumor-bearing mice (tumor site indicated by red arrow). Reproduced with permission.<sup>[85]</sup> Copyright 2018, Royal Society of Chemistry.

model showed a promising synergistic therapy outcome. Delivering DOX to tumor cells was also reported by using unilamellar micelles (UMs) covalently conjugated with DOX via an acid-cleavable hydrazone linker.<sup>[62]</sup> UMs of diblock copolymer poly(2-methoxy-2-oxoethyl methacrylate)-*b*-poly[(ethylene glycol) methyl ether methacrylate]) extended from a  $\beta$ -cyclodextrin core were sensitive to acidic pH. The system showed fast DOX release in vitro with decreasing pH, and the intrinsic fluorescence of DOX once cleaved from the polymer was used to monitor the cellular internalization, activation of the prodrug and the delivery to the nucleus via lysosomes. The UMs showed higher toxicity to HeLa (tumor) cells in vitro than to human endothelial cells. However, in vivo experiments were not conducted, which would be necessary to prove their antitumor effect. Uniformly-disperse micelles with an average size of 80 nm were assembled from bis-

condensed dicyanomethylene-4*H*-pyran (DCM) and a PEG conjugated with biotin for active targeting. DCM serving for imaging by NIR fluorescence was conjugated with the anticancer prodrug camptothecin through a GSH-responsive disulfide-bond. These micelles displayed a selective tumor accumulation and drug release through the EPR effect and biotin interaction. Very high inhibition rates of tumor growth of nearly 99.7% in HeLa tumor-bearing nude mice were obtained with this theranostic assembly (Figure 5).<sup>[85]</sup>

## 7.2. Dual Stimuli-Responsiveness of Polymer Assemblies

In order to obtain an enzyme-responsive system, an amphiphilic random copolyester consisting of *N*-protected L-aspartic acid,



1,12-dodecanediol, and triethyleneglycol formed micelles of sizes less than 200 nm in aqueous medium and exhibited excellent coencapsulation efficiency for the anti-inflammatory drug curcumin and Nile Red (NR), a fluorescent dye. This ester bond-based polymer is of interest since it can be hydrolyzed by esterases under ambient conditions. The micelles demonstrated a high extracellular stability while they quickly degraded in the intracellular environment due to the presence of enzymes. With FRET between curcumin and NR, endocytosis and enzymatic degradation could be followed by the onset of NR fluorescence. In addition, the micelles were successful in killing almost 90% of breast cancer cells *in vitro*.<sup>[63]</sup>

Magnetic-responsive theranostics can be used in a different manner than magnetic hyperthermia. For example, micelles based on biocompatible hybrid calcium phosphate PEG-*b*-polyanion and containing Gd(III) chelates served for image-guided gadolinium neutron capture tumor therapy.<sup>[40]</sup> Colloidal stabilization of Gd-diethylenetriaminepentaacetic acid (Gd-DTPA) as hybrid micelles yielded higher molecular relaxivity and an improved kill rate toward murine colon adenocarcinoma cells under thermal neutron irradiation (TNI). More importantly, no further tumor cell proliferation could be observed after TNI. Future design improvements are expected to bring spatial-temporal control of outwardly-displayed chemical moieties based on polymer LCST<sup>[84]</sup> or could very well take inspiration from magneto-activated stromatocytes<sup>[132]</sup> for capturing and releasing nanoparticles.

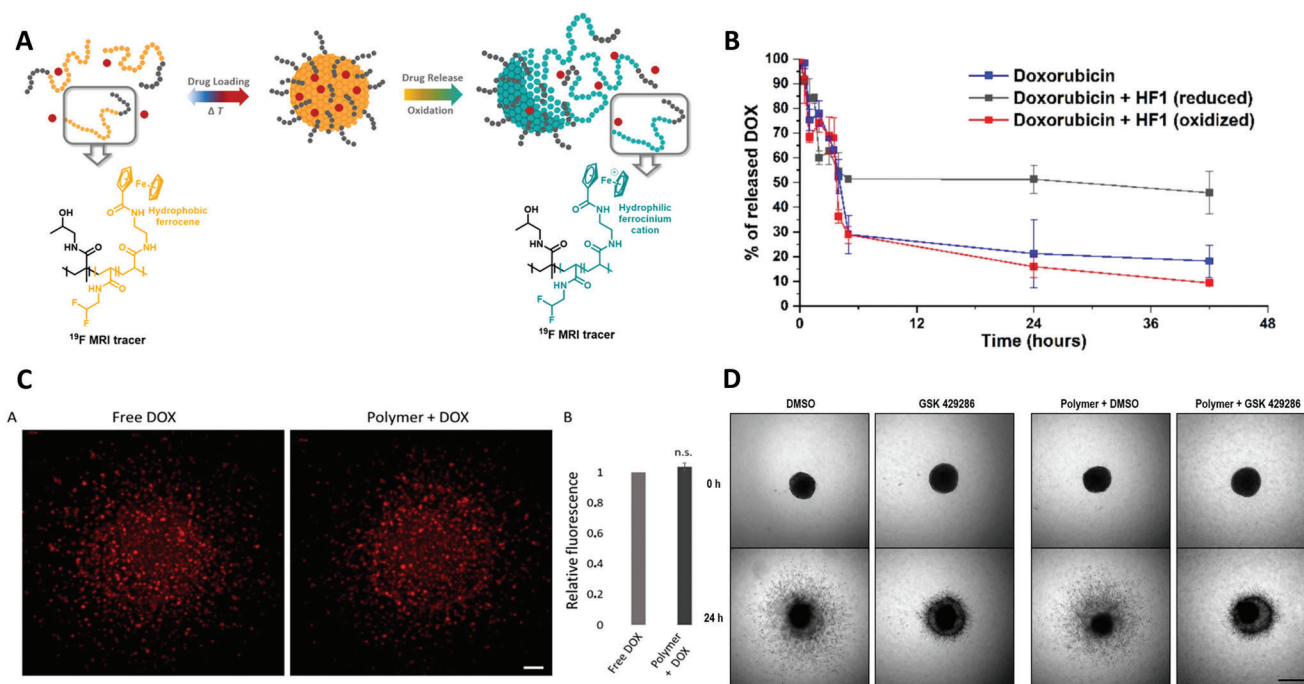
GSH, which is the main cellular redox buffer,<sup>[133]</sup> was selected as a stimulus for poly(ethylene glycol-*b*-poly(propylene sulfide)-*SS*-poly(ethylene glycol) PEG-PPS-*SS*-PEG polymersomes, containing a GSH-cleavable disulfide bond.<sup>[64]</sup> The polymersomes were loaded with ultrasmall paramagnetic iron oxide nanoparticles (USPIONS) coated with PAA and DOX. DOX was stabilized by electrostatic interactions with PAA and complexation with the Fe ions of USPIONS. Upon cellular uptake and GSH exposure, the *SS* bonds were cleaved, inducing an architectural change to micelles and the eventual release of the drug and activation of the T<sub>1</sub> MRI contrast agent (USPIONS) due to an unrestricted water penetration compared to the situation when USPIONS were coated with PAA and DOX. The theranostic system was evaluated both in a human colorectal carcinoma and lung cancer cell model and in an *in vivo* mouse model. This system elegantly combines therapeutic and diagnostic activation, which are both stimulated by the same trigger.

A polymersome that is surface-functionalized with an aptamer represents an attractive and elegant strategy to target tumor sites. In this regard, the AS1411 DNA aptamer was selected for its high affinity to nucleolin, a protein overexpressed on the surface of breast, colon, lung, prostate, and gastric cancer cells. Polymersomes of PEG-*b*-PCL were loaded with DOX and hydrophobic quantum dots (QDs) based on indium-copper-gadolinium-zinc sulfide (APT-DOX-QD-NP) and then conjugated with AS1411 DNA aptamer. QDs served as an MR and fluorescence contrast agent and showed that the theranostic platform efficiently and selectively accumulates in an implemented 4T1 tumor in BALB/c mice.<sup>[30]</sup>

A smart combination of temperature-induced release of a model compound, actively controlled by an external magnetic field through the incorporation of SPIONS, was

achieved for polymersomes based on poly(isoprene)-*b*-poly(*N*-isopropylacrylamide) (PI-*b*-PNIPAM). SPIONS were embedded into the polymersome membrane while calcein, a hydrophilic dye, was encapsulated in the lumen. Upon the application of an alternating magnetic field, heat is generated and a reversible structural change in the polymersomes occurred and permeabilized the membrane such to release calcein as a proof of principle for small molecules release.<sup>[33]</sup> Polymersomes have also been loaded with magnetic-sensitive nanomaterials. The therapeutics release is tuned by encapsulating the magnetic nanomaterials in the membrane of polymersomes. Featuring almost 70 wt% of maghemite in the bilayer, polymersomes built on biodegradable block copolymers and loaded with DOX, were made highly deformable under an applied magnetic field and provided an improved MRI contrast.<sup>[43]</sup> Another combination of stimuli was achieved by introducing redox-responsive ferrocene moieties into a temperature-responsive fluorine-enriched amphiphilic block copolymer (**Figure 6**).<sup>[81]</sup> This approach provides a more sophisticated dual responsive system with a sharp signal in <sup>19</sup>F MRI. The polymeric theranostic tracer forms spherical particles (nanogels) upon heating above 33 °C but disassembles when exposed to oxidative conditions. The capability to load and deliver the drugs upon exposure to different stimuli along with the ability to visualize the therapeutic effects of the released drugs emphasize the significant potential of this strategy in designing advanced theranostics for more efficient clinical treatments.

An interesting example for the combination of exogenous (sonication) and endogenous (ROS) stimuli is given by core-shell nanoparticles, composed of a polymeric dextran-*p*(OEGMA)<sub>9</sub>-*b*-*p*(MTEMA)<sub>22</sub> core, coloaded with DOX as the therapeutic moiety and a sonosensitizer as the diagnostic moiety.<sup>[82]</sup> For high loading efficiency and bioavailability, the core particles were encapsulated into the shell composed of a red blood cell-derived, peptide-modified membrane. By the combination of both exogenous and endogenous stimuli, a controlled DOX release after cellular uptake was achieved. Sonication allowed for ROS generation (singlet oxygen) from endogenous H<sub>2</sub>O<sub>2</sub>, leading to the destabilization of the polymeric carrier based on the thioether. In another example, PEG was used in a polymeric pH- and GSH-responsive micelle composed of mPEG-*SS*-poly((2-azepane ethyl methacrylate)-*co*-TBIS) (mPEG-*SS*-poly(AEMA-*co*-TBIS) as a promising system for two-photon cell and tissue bioimaging and chemotherapy. In this regard, TBIS, which is a triphenylamine derivative, was used as a fluorophore to provide aggregation-induced emission activity, DOX was encapsulated as a therapeutic agent and PAEMA and the disulfide bonds served as a pH and GSH response by the tumor microenvironment.<sup>[134]</sup> pH and temperature dual responsiveness was also achieved with PNIPAM-PDOPA micelles with encapsulated DOX, which served as a therapeutic drug and diagnostic agent simultaneously due to its inherent fluorescence.<sup>[135]</sup> Catechol units of L-DOPA were complexed with Fe(III) ions at physiological pH, whereas when lowering to pH 5, the biscomplex destabilizes into a mono-complex. The micelles showed enhanced *in vitro* release of DOX with increasing temperature and decreasing pH, as well as cytotoxicity and accumulation via the EPR effect in the tumor. However, the system accumulated in the liver, kidney, and testis as well, indicating that a targeting strategy is necessary.



**Figure 6.** A) Dual stimuli-responsive diblock copolymer PHPMA-*b*-P(DFEA-*stat*-FcCEA) assemble into spherical particles (nanogels) upon heating to physiological temperature because of the LCST of PDFEA block and can be loaded with different hydrophobic drugs (e.g., GSK 429286, Rho kinase inhibitor). Drug release (DOX) is achieved through the responsiveness of ferrocene (PFcCEA) to intracellularly risen ROS levels in cancer cells. The polymeric backbone containing fluorine is used as a tracer for <sup>19</sup>F MRI. B) DOX release study in vitro, showing that the reduced ferrocene is able to hold back the drug more efficiently over time than the oxidized form. C) Distribution study in 3D spheroidal clusters of HT1080 cancer cells with (A) free DOX and (B) DOX-loaded polymer NPs, showing successful penetration of the NPs with no significant difference to the free DOX control (Student's *t*-test). Signal shows the measured DOX fluorescence intensity. D) In vitro spheroid proliferation study of HT1080 cancer cells, showing the successful inhibition of tumor proliferation by drug exposure as well as by drug encapsulated in polymer NPs, as compared to high proliferation in controls, indicating again successful penetration of particles into tumor tissue as well as efficient drug release of the polymer NPs in tumor environment and (scale bar: 500 μm). Reproduced (with permission.<sup>[81]</sup> Copyright 2021, American Chemical Society.

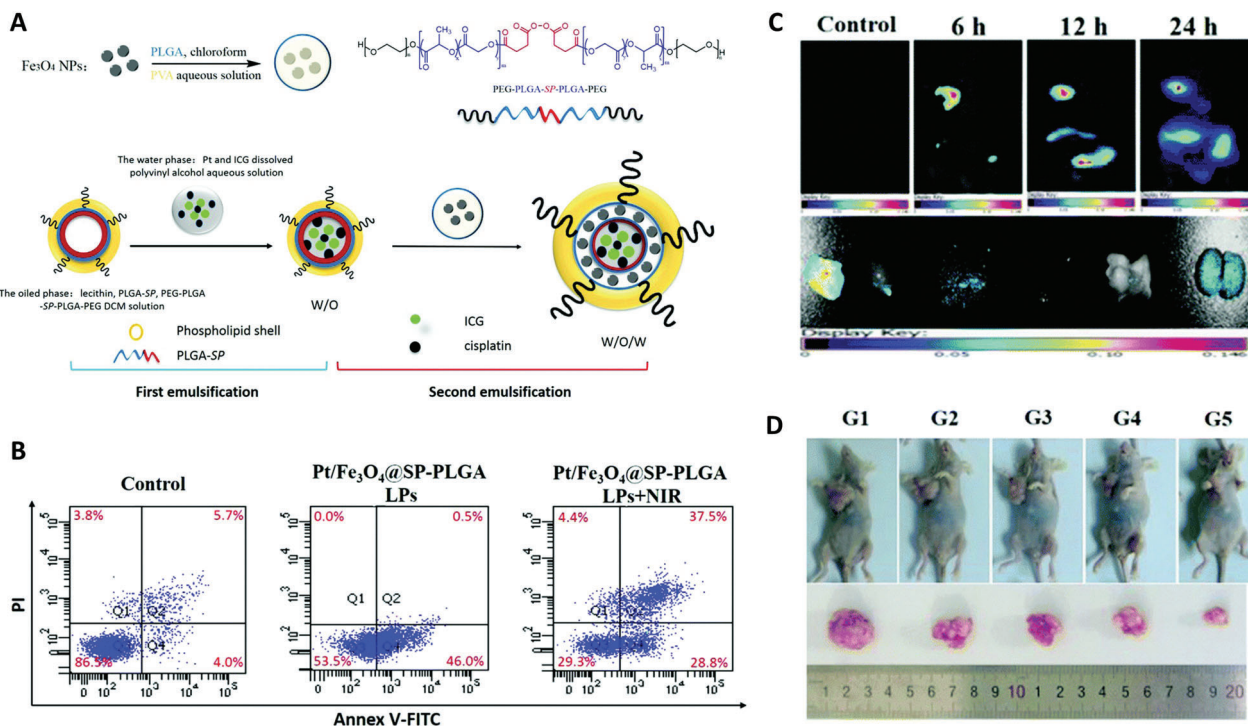
Micelles were even used for a multiresponsive system, as they were able to respond to three different stimuli (pH, temperature, and redox). Micelles loaded with DOX were assembled from a triblock copolymer consisting of pH-responsive PLys and thermoresponsive PNIPAM, tethered by a redox-responsive disulfide linker to biodegradable PCL (PNIPAM<sub>30</sub>-SS-*b*-PLys<sub>30</sub>-*b*-PCL<sub>n</sub>).<sup>[179]</sup> The triple-stimuli responsiveness allowed for 85% drug release at pH 5.0, 42 °C, in presence of 10 mM GSH. In vivo and *ex vivo* biodistribution studies revealed that after 72 h, the highest DOX concentration was in the tumor, followed by the liver. This example shows that passive targeting relying on the EPR effect combined with tumor-specific triple-stimuli responsiveness can be a successful strategy to efficiently target tumors. In a different approach, chitosan-based polymers were used to self-assemble into multiresponsive micelles for theranostic systems.<sup>[136]</sup> For example, folic acid-conjugated carboxymethyl lauryl chitosan formed hybrid micelles in the presence of hydrophobic SPIONs, exhibiting a pH-triggered release of the encapsulated drug, camptothecin, and active targeting due to the presence of folic acid.<sup>[137]</sup> SPIONs served both for imaging the region of interest and to enhance the tumor-targeted delivery of the drug in vivo when an external magnetic field was applied.

A novel chemodynamic therapy that has attracted considerable attention is the use of a Fenton reaction, thereby aiming to generate ROS, triggered by external NIR irradiation and acidic tu-

mor environment, which in return has a tumor cell killing effect. In this regard, succinic acid peroxide is bound to poly(ethylene glycol)-*b*-(poly(lactic-*co*-glycolic acid)), and the resulting (PEG-PLGA)<sub>2</sub>-SP copolymer is self-assembled in the presence of iron oxide NPs 8 nm in size that react together and generate <sup>1</sup>O<sub>2</sub>. The theranostics system is generated through double emulsion, where iron oxide NPs were emulsified with encapsulated cisplatin and indocyanine green (ICG) as fluorescence dye in a lipo-polymerosome blend based on PLGA, grafted with SP and mixed with lecithin, namely, Pt/Fe<sub>3</sub>O<sub>4</sub>@SP-PLGA LPs. The ROS-mediated oxidation of the theranostics platform induced significant cell death in vitro and inhibited the MCF-7 tumor growth in vivo (Figure 7).<sup>[138]</sup>

## 8. Polymer Theranostic Systems with More Complex Architecture/Properties

In order to achieve improved properties or provide better functionality, assemblies with more complex architecture/properties have been developed. A step forward was thus achieved by introducing multicompart ment theranostics, an emerging trend in nanomedicine. This novel concept uses multimodular/multicompart ment architecture of the assemblies, where the diagnostic elements are spatially segregated from the therapeutics-loaded compartments. In nature, nanoscale



**Figure 7.** A) Preparation of lipo-polymersomes (Pt/Fe<sub>3</sub>O<sub>4</sub>@SP-PLGA LPs) and encapsulation of cisplatin, ICG, and Fe<sub>3</sub>O<sub>4</sub> via double-emulsion. B) Apoptosis investigation in MCF-7 cells treated with Pt/Fe<sub>3</sub>O<sub>4</sub>@SP-PLGA. Treatment with LPs alone leads to an increase in the apoptotic cell portion (Q4), and additional NIR irradiation increased the portion of dead cells. C) In vivo fluorescence images of MCF-7 breast tumor-bearing nude mice treated with an intratumoral injection of LPs and in situ fluorescence images of dissected organs of mice 24 h after injection. D) Photographs of MCF-7 breast tumor-bearing mice treated with PBS solution (G1), Fe<sub>3</sub>O<sub>4</sub>@PLGA (G2), Fe<sub>3</sub>O<sub>4</sub>@SP-PLGA (G3), Pt/Fe<sub>3</sub>O<sub>4</sub>@SP-PLGA (G4), and Pt/Fe<sub>3</sub>O<sub>4</sub>@SP-PLGA + NIR (G5). Reproduced with permission.<sup>[138]</sup> Copyright 2019, Royal Society of Chemistry.

compartmentalization is essential as it allows for the separation of biochemical reactions in cells.<sup>[139]</sup> Multicompartmentalization can be principally achieved by forming clusters of similarly sized nanocompartments that are physically or chemically linked to each other. These spatially segregated nanocompartments can be loaded with catalytic, therapeutic, and imaging agents. This new class of theranostics could allow scientists to overcome the shortcomings of single systems by having multiple imaging agents and various therapeutics loaded in the same carrier.<sup>[140]</sup> Polymersome clusters can be generated by using specific linkers between the nanocompartments, mainly using molecular recognition interactions. For example, polymersomes exposing ssDNA and complementary ssDNA, respectively, have been zipped together due to DNA hybridization.<sup>[141]</sup> Such polymersome clusters provide an elegant manner to selectively load each compartment with a specific, segregated cargo, thus enabling the dual functionality required for theranostic systems. The polymersome clusters solve the usual drawbacks of single loaded-polymersomes, such as inactivation of sensitive enzymes by imaging agents or inorganic nanoparticles.<sup>[141]</sup>

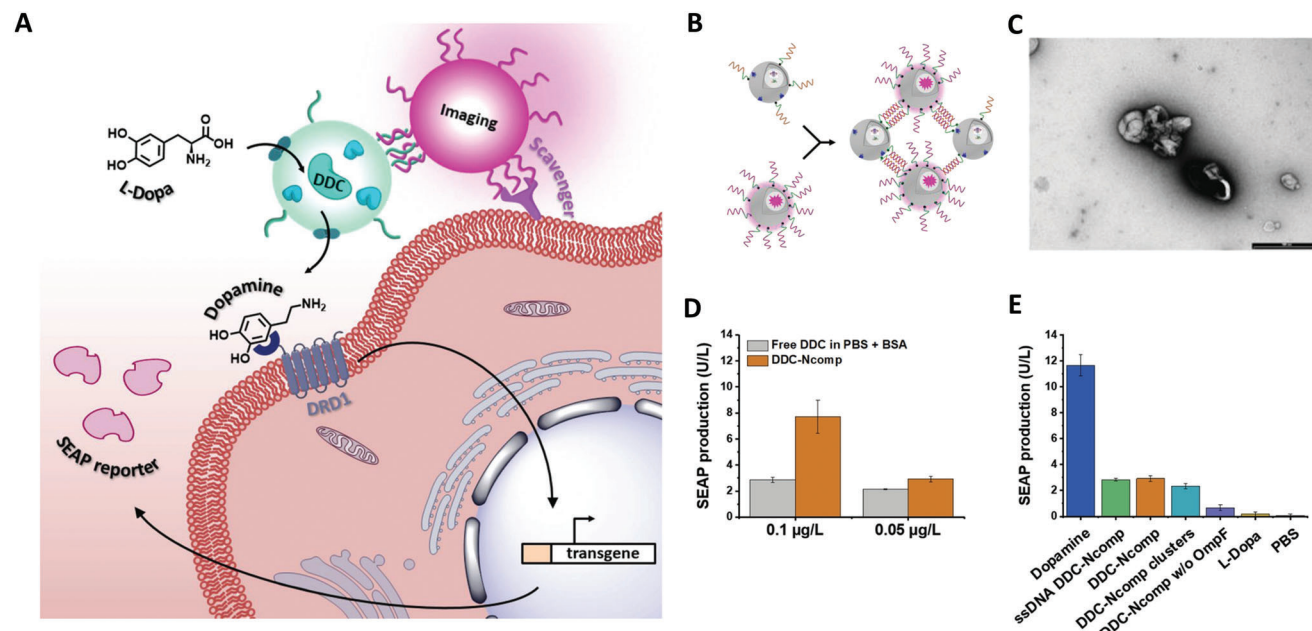
A multicompartment theranostic system for atherosclerosis diagnosis and therapy composed of polydimethylsiloxane-*block*-poly(2-methyl-2-oxazoline) (PDMS-*b*-PMOXA) polymersome clusters was designed through the combination of a “diagnostic compartment” loaded with fluorescent DY-633 and a “therapeutic compartment.”<sup>[16]</sup> The therapeutic polymersome was loaded with human enzyme DOPA decarboxylase (DDC) and equipped

with outer membrane porin F (OmpF) from *Escherichia coli* to guarantee membrane permeability. As there were still nonhybridized ssDNA strands remaining after the cluster formation, they served for specific interactions with scavenger receptors of engineered cells. The clusters were functional as they produced dopamine as reported by the detectable reporter enzyme secreted, embryonic alkaline phosphatase, and simultaneously allowed one to visualize their localization by the fluorescent intensity associated with the presence of DY-633 (Figure 8).<sup>[16]</sup>

A different approach toward coencapsulation was realized by superassemblies as they combine a separation of nanocompartments with the availability of complementary functions. These types of superassemblies were mostly based on inorganic nanoparticle clusters: gold nanorods with NaGdF<sub>4</sub> particles as the imaging modality or drug-loaded nanoparticles with gold nanoparticles as systems for imaging and chemothermal therapy in one.<sup>[36,142]</sup>

## 9. Conclusion

The development of theranostic systems is a major focus today due to the need to improve the patient experience by offering efficient solutions for diagnostics and therapeutics. The early detection of pathologic conditions and simultaneous treatment is crucial to decrease side effects and increase the chances of cure. In this review, we present recent advances of polymer-based nanoassemblies with a focus on stimuli-responsive



**Figure 8.** A) Illustration of the cellular mechanism of theranostic polymersome clusters zipped by complementary ssDNA, composed of therapeutic compartments containing DOPA decarboxylase (DDC) and diagnostic compartments containing fluorescent DY-633 dye. DDC catalyzes the conversion of L-DOPA into dopamine, which triggers the gene expression of secreted embryonic alkaline phosphatase (SEAP) reporter enzyme in cells via activation of dopamine receptors D1 (DRD1). Excess ssDNA leads to binding of the nanotheranostic platform to epithelial cells via interaction with scavenger receptors. B) Formation of a theranostic cluster by DNA hybridization. C) TEM image of polymersome clusters (scale bar: 500 nm). D) Cellular production of SEAP is dependent on the concentration of therapeutic polymersomes or free DDC. E) Cellular expression of SEAP after treatment with theranostic nanocompartments and controls. Reproduced with permission.<sup>[16]</sup> Copyright 2020, Wiley-VCH.

systems that are considered more efficient because they allow for better control of the cargo delivery. In addition, we include selected examples of other theranostic systems with more complex architecture (e.g., multicompartments). Starting with the variety of endogenous and exogenous stimuli, we indicate how systems based on polymer nanoassemblies, if necessary tailored by combination with various inorganic nanoparticles, serve as carriers for therapeutic molecules and “reporting” molecules/nano-objects (e.g., metallic nanoparticles, nanorods). We selected recent examples to indicate how such assemblies are generated and how they respond to one or more stimuli to control their delivery and overall efficiency in specific biolocations and conditions. As polymer-based theranostic systems are gaining increasing attention, there are still open questions to solve in their production to achieve the desired properties in terms of stimuli-responsiveness, biocompatibility, bioavailability, biodegradation, biodistribution, and elimination from the body. Since covalent functionalization of polymers or ligands, incorporation of conjugated reporting nano-objects, or postfunctionalization with targeting molecules often requires multistep synthesis, such theranostic systems need significant optimization steps, resulting in an increase of their production costs, especially for the potential use in patients on a larger scale. As different compounds or nano-objects (e.g., inorganic nanoparticles), which are incorporated in one single carrier, can mutually affect their properties and functionality by physicochemical interaction with the self-assembled structure, or can have unexpected synergistic effects in vivo, the effect of coentrapment still has to be addressed in more systematic studies. In order to advance as viable theranostic systems, the

polymer-based nanoassemblies should be optimized in terms of stability, entrapment, and release efficiency. In addition, further studies are necessary to address disease-specific issues and suggest solutions compatible with individualized medicine. At the same time, theranostic systems should allow a straightforward change of components supporting a broader applicability of the platform in order to be cost-efficient. One potential approach to reach this purpose is a modular system, where various building constituents with distinct functions and effects can be interchanged, depending on the patient’s health history or disease specificity. While the design of multicompartment systems represents a very promising approach, such assemblies have to be carefully controlled to limit their size for the desired application (intra- or intercellular). Even though they are in the early stages of research, there are already examples of in vivo assays indicating the high potential of these theranostic approaches. However, the number of such assays should be significantly increased to understand the fate of the therapeutics in vivo and evaluate their overall efficiency. In addition, efforts need to be made to study their toxicity as well as their biodegradability or elimination from various biological entities. Addressing these open questions will support the development of efficient theranostic systems as an improved means of patient care.

## Acknowledgements

The authors gratefully acknowledge the financial support provided by the Swiss National Science Foundation, the University of Basel, and the National Centre of Competence in Research – Molecular

Systems Engineering (NCCR-MSE). The authors thank Dr. Olivia Eggenberger (University of Basel) for editing the manuscript. Figure 1 and ToC image were created with BioRender.com.

Open access funding provided by CSAL - Universitat Basel.

## Conflict of Interest

The authors declare no conflict of interest.

## Author Contributions

C.G.P.: conceptualization, project administration, and supervision. C.G.P.: funding acquisition. M.M., P.K., A.D., D.N., and C.J.: literature search and article selection. M.M., P.K., D.N., and C.J.: writing the original draft. M.M., P.K., A.D., and C.G.P.: writing and reviewing. M.M., P.K., A.D., and C.G.P.: writing the finalization of manuscript. M.M.: design of Figure 1 and TOC image.

## Keywords

inorganic nanoparticles, self-assembly, stimuli-responsiveness, synthetic polymers, theranostics

Received: June 30, 2022

Revised: August 28, 2022

Published online: September 26, 2022

- [1] A. Vaidya, Y. Sun, T. Ke, E. K. Jeong, Z. R. Lu, *Magn. Reson. Med.* **2006**, *56*, 761.
- [2] P. Juzenas, W. Chen, Y. P. Sun, M. A. Coelho, R. Generalov, N. Generalova, I. L. Christensen, *Adv. Drug Delivery Rev.* **2008**, *60*, 1600.
- [3] K. Park, S. Lee, E. Kang, K. Kim, K. Choi, I. C. Kwon, *Adv. Funct. Mater.* **2009**, *19*, 1553.
- [4] G. Orive, O. A. Ali, E. Anitua, J. L. Pedraz, D. F. Emerich, *Biochim. Biophys. Acta* **2010**, *1806*, 96.
- [5] K. Y. Choi, G. Liu, S. Lee, X. Chen, *Nanoscale* **2012**, *4*, 330.
- [6] B. T. Luk, L. Zhang, *ACS Appl. Mater. Interfaces* **2014**, *6*, 21859.
- [7] W. Zhang, W. Wang, D. X. Yu, Z. Xiao, Z. He, *Nanomedicine* **2018**, *13*, 2341.
- [8] S. Shakeri, M. Ashrafzadeh, A. Zarrabi, R. Roghanian, E. G. Afshar, A. Pardakhty, R. Mohammadnejad, A. Kumar, V. K. Thakur, *Biomedicines* **2020**, *8*, 13.
- [9] J. Tang, M. E. Lobatto, J. C. Read, A. J. Mieszawska, Z. A. Fayad, W. J. Mulder, *Curr. Cardiovasc. Imaging Rep.* **2012**, *5*, 19.
- [10] A. M. Flores, J. Ye, K. U. Jarr, N. Hosseini-Nassab, B. R. Smith, N. J. Leeper, *Arterioscler., Thromb., Vasc. Biol.* **2019**, *39*, 635.
- [11] J. Bejarano, M. Navarro-Marquez, F. Morales-Zavala, J. O. Morales, I. Garcia-Carvajal, E. Araya-Fuentes, Y. Flores, H. E. Verdejo, P. F. Castro, S. Lavandero, M. J. Kogan, *Theranostics* **2018**, *8*, 4710.
- [12] M. K. Gupta, Y. Lee, T. C. Boire, J. B. Lee, W. S. Kim, H. J. Sung, *Nanotheranostics* **2017**, *1*, 166.
- [13] D. P. Cormode, G. O. Skajaa, A. Delshad, N. Parker, P. A. Jarzyna, C. Calcagno, M. W. Galper, T. Skajaa, K. C. Briley-Saebo, H. M. Bell, R. E. Gordon, Z. A. Fayad, S. L. Woo, W. J. Mulder, *Bioconjugate Chem.* **2011**, *22*, 353.
- [14] M. Howell, C. Wang, A. Mahmoud, G. Hellermann, S. S. Mohapatra, S. Mohapatra, *Drug Delivery Transl. Res.* **2013**, *3*, 352.
- [15] Y. Wu, R. Zhang, H. D. N. Tran, N. D. Kurniawan, S. S. Moonshi, A. K. Whittaker, H. T. Ta, *ACS Appl. Nano Mater.* **2021**, *4*, 3604.
- [16] C. E. Meyer, J. Liu, I. Craciun, D. Wu, H. Wang, M. Xie, M. Fussenegger, C. G. Palivan, *Small* **2020**, *16*, 1906492.
- [17] O. P. Singh, M. R. Gedda, S. L. Mudavath, O. N. Srivastava, S. Sundar, *Nanomedicine* **2019**, *14*, 1911.
- [18] N. Hoshyar, S. Gray, H. Han, G. Bao, *Nanomedicine* **2016**, *11*, 673.
- [19] S. Nejadi, E. M. Vadeghani, S. Khorshidi, A. Karkhaneh, *Eur. Polym. J.* **2020**, *122*, 109353.
- [20] Y. Shi, R. van der Meel, X. Chen, T. Lammers, *Theranostics* **2020**, *10*, 7921.
- [21] Y. Xu, H. Wu, J. Huang, W. Qian, D. E. Martinson, B. Ji, Y. Li, Y. A. Wang, L. Yang, H. Mao, *Theranostics* **2020**, *10*, 2479.
- [22] P. Ofek, K. Miller, A. Eldar-Boock, D. Polyak, E. Segal, R. Satchi-Fainaro, *Isr. J. Chem.* **2010**, *50*, 185.
- [23] M. Ohlson, J. Sorensson, B. Haraldsson, *Am. J. Physiol. Renal. Physiol.* **2001**, *280*, F396.
- [24] K. C. Black, Y. Wang, H. P. Luehmann, X. Cai, W. Xing, B. Pang, Y. Zhao, C. S. Cutler, L. V. Wang, Y. Liu, Y. Xia, *ACS Nano* **2014**, *8*, 4385.
- [25] T. J. Liu, L. L. Tong, N. N. Lv, X. G. Ge, Q. R. Fu, S. Gao, Q. E. Ma, J. B. Song, *Adv. Funct. Mater.* **2019**, *29*, 1806429.
- [26] F. Mahmoodzadeh, M. Abbasian, M. Jaymand, R. Salehi, E. Bagherzadeh-Khajehmarjan, *Mater. Sci. Eng., C* **2018**, *93*, 880.
- [27] Y.-T. Qin, H. Peng, X.-W. He, W.-Y. Li, Y.-K. Zhang, *ACS Appl. Mater. Interfaces* **2019**, *11*, 34268.
- [28] Y. Zhuang, L. Zhao, L. Zheng, Y. Hu, L. Ding, X. Li, C. Liu, J. Zhao, X. Shi, R. Guo, *ACS Biomater. Sci. Eng.* **2017**, *3*, 431.
- [29] D. Ling, W. Park, S. J. Park, Y. Lu, K. S. Kim, M. J. Hackett, B. H. Kim, H. Yim, Y. S. Jeon, K. Na, T. Hyeon, *J. Am. Chem. Soc.* **2014**, *136*, 5647.
- [30] T. Zavvar, M. Babaei, K. Abnous, S. M. Taghdisi, S. Nekooei, M. Ramezani, M. Alibolandi, *Int. J. Pharm.* **2020**, *578*, 119091.
- [31] H. Deng, Y. Zhong, M. Du, Q. Liu, Z. Fan, F. Dai, X. Zhang, *Theranostics* **2014**, *4*, 904.
- [32] Y. Liu, Z. Yang, X. Huang, G. Yu, S. Wang, Z. Zhou, Z. Shen, W. Fan, Y. Liu, M. Davissou, H. Kalish, G. Niu, Z. Nie, X. Chen, *ACS Nano* **2018**, *12*, 8129.
- [33] O. Bixner, S. Kurzhals, M. Virk, E. Reimhult, *Materials* **2016**, *9*, 29.
- [34] K. Hayashi, M. Nakamura, H. Miki, S. Ozaki, M. Abe, T. Matsumoto, W. Sakamoto, T. Yogo, K. Ishimura, *Theranostics* **2014**, *4*, 834.
- [35] K. Hayashi, Y. Sato, W. Sakamoto, T. Yogo, *ACS Biomater. Sci. Eng.* **2017**, *3*, 95.
- [36] M. Sun, L. Xu, W. Ma, X. Wu, H. Kuang, L. Wang, C. Xu, *Adv. Mater.* **2016**, *28*, 898.
- [37] Q. Ren, K. Yang, R. Zou, Z. Wan, Z. Shen, G. Wu, Z. Zhou, Q. Ni, W. Fan, J. Hu, Y. Liu, *Nanoscale* **2019**, *11*, 23021.
- [38] D. H. Nguyen, J. S. Lee, J. H. Choi, K. M. Park, Y. Lee, K. D. Park, *Acta Biomater.* **2016**, *35*, 109.
- [39] J. R. Upponi, K. Jerajani, D. K. Nagesha, P. Kulkarni, S. Sridhar, C. Ferris, V. P. Torchilin, *Biomaterials* **2018**, *170*, 26.
- [40] P. Mi, N. Dewi, H. Yanagie, D. Kokuryo, M. Suzuki, Y. Sakurai, Y. Li, I. Aoki, K. Ono, H. Takahashi, H. Cabral, N. Nishiyama, K. Kataoka, *ACS Nano* **2015**, *9*, 5913.
- [41] N. D. Thorat, R. A. Bohara, M. R. Noor, D. Dhamecha, T. Soulimane, S. A. M. Tofail, *ACS Biomater. Sci. Eng.* **2017**, *3*, 1332.
- [42] Y. Hao, L. Wang, B. Zhang, H. Zhao, M. Niu, Y. Hu, C. Zheng, H. Zhang, J. Chang, Z. Zhang, Y. Zhang, *Nanotechnology* **2016**, *27*, 025101.
- [43] C. Sanson, O. Diou, J. Thevenot, E. Ibarboue, A. Soum, A. Brulet, S. Miraux, E. Thiaudiere, S. Tan, A. Brisson, V. Dupuis, O. Sandre, S. Lecommandoux, *ACS Nano* **2011**, *5*, 1122.
- [44] M. Adabi, M. Naghibzadeh, M. Adabi, M. A. Zarrinfard, S. S. Esnaashari, A. M. Seifalian, R. Faridi-Majidi, H. Tanimowo Aiye-labegan, H. Ghanbari, *Artif. Cells, Nanomed., Biotechnol.* **2017**, *45*, 833.
- [45] E. Calzoni, A. Cesaretti, A. Polchi, A. Di Michele, B. Tancini, C. Emiliani, *J. Funct. Biomater.* **2019**, *10*, 4.
- [46] X. M. Li, L. Wang, Y. B. Fan, Q. L. Feng, F. Z. Cui, *J. Nanomater.* **2012**, *2012*, 6.

- [47] S. Ghosh, R. Lalani, V. Patel, D. Bardoliwala, K. Maiti, S. Banerjee, S. Bhowmick, A. Misra, *J. Controlled Release* **2019**, 296, 114.
- [48] D. Patra, P. Kumar, T. K. Dash, I. Chakraborty, R. Bhattacharyya, R. Shunmugam, *ACS Appl. Polym. Mater.* **2022**, 4, 1752.
- [49] D. Patra, S. Mukherjee, I. Chakraborty, T. K. Dash, S. Senapati, R. Bhattacharyya, R. Shunmugam, *ACS Biomater. Sci. Eng.* **2018**, 4, 1738.
- [50] Z. Yang, L. Li, A. J. Jin, W. Huang, X. Chen, *Mater. Horiz.* **2020**, 7, 1474.
- [51] M. Elsabahy, G. S. Heo, S. M. Lim, G. Sun, K. L. Wooley, *Chem. Rev.* **2015**, 115, 10967.
- [52] F. Wang, J. Xiao, S. Chen, H. Sun, B. Yang, J. Jiang, X. Zhou, J. Du, *Adv. Mater.* **2018**, 30, 1705674.
- [53] K. Ulbrich, K. Hola, V. Subr, A. Bakandritsos, J. Tucek, R. Zboril, *Chem. Rev.* **2016**, 116, 5338.
- [54] Z. Wang, G. Niu, X. Chen, *Pharm. Res.* **2014**, 31, 1358.
- [55] A. J. Sivaram, P. Rajitha, S. Maya, R. Jayakumar, M. Sabitha, *Wiley Interdiscip. Rev.: Nanomed. Nanobiotechnol.* **2015**, 7, 509.
- [56] Ł. Lamch, A. Pucek, J. Kulbacka, M. Chudy, E. Jastrzębska, K. Tokarska, M. Bułka, Z. Brzózka, K. A. Wilk, *Adv. Colloid Interface Sci.* **2018**, 261, 62.
- [57] N. Haider, S. Fatima, M. Taha, M. Rizwanullah, J. Firdous, R. Ahmad, F. Mazhar, A. M. Khan, *Curr. Pharm. Des.* **2020**, 26, 1216.
- [58] Y. Wang, H. Zhang, Z. Wang, L. Feng, *ACS Appl. Polym. Mater.* **2020**, 2, 4222.
- [59] A. B. Cook, P. Decuzzi, *ACS Nano* **2021**, 15, 2068.
- [60] Z. Z. Fang, Y. F. Shen, D. Q. Gao, *New J. Chem.* **2021**, 45, 4534.
- [61] C. F. de Freitas, E. Kimura, A. F. Rubira, E. C. Muniz, *Mater. Sci. Eng., C* **2020**, 112, 110853.
- [62] X. Shi, M. Hou, S. Bai, X. Ma, Y. E. Gao, B. Xiao, P. Xue, Y. Kang, Z. Xu, C. M. Li, *Mol. Pharmaceutics* **2017**, 14, 4032.
- [63] S. Saxena, A. Pradeep, M. Jayakannan, *ACS Appl. Bio Mater.* **2019**, 2, 5245.
- [64] D. Liu, Z. Zhou, X. Wang, H. Deng, L. Sun, H. Lin, F. Kang, Y. Zhang, Z. Wang, W. Yang, L. Rao, K. Yang, G. Yu, J. Du, Z. Shen, X. Chen, *Biomaterials* **2020**, 244, 119979.
- [65] J. Leong, J. Y. Teo, V. K. Aakalu, Y. Y. Yang, H. Kong, in *Adv. Healthcare Mater.*, **2018**, p. 7/1701276.
- [66] J. Kaur, V. Mishra, S. K. Singh, M. Gulati, B. Kapoor, D. K. Chellappan, G. Gupta, H. Dureja, K. Anand, K. Dua, G. L. Khatik, K. Gowthamarajan, *J. Controlled Release* **2021**, 334, 64.
- [67] V. I. Martynov, A. A. Pakhomov, I. E. Deyev, A. G. Petrenko, *Biochim. Biophys. Acta, Gen. Subj.* **2018**, 1862, 2924.
- [68] P. Swietach, R. D. Vaughan-Jones, A. L. Harris, A. Hulikova, *Philos. Trans. R. Soc., B* **2014**, 369, 20130099.
- [69] E. Georgieva, D. Ivanova, Z. Zhelev, R. Bakalova, M. Gulubova, I. Aoki, *Anticancer Res.* **2017**, 37, 5373.
- [70] F. Q. Schafer, G. R. Buettner, *Free Radical Biol. Med.* **2001**, 30, 1191.
- [71] S. Quintero-Fabián, R. Arreola, E. Becerril-Villanueva, J. C. Torres-Romero, V. Arana-Argáez, J. Lara-Riegos, M. A. Ramírez-Camacho, M. E. Alvarez-Sánchez, *Front. Oncol.* **2019**, 9, 1370.
- [72] H. Tang, Y. Guo, L. Peng, H. Fang, Z. Wang, Y. Zheng, H. Ran, Y. Chen, *ACS Appl. Mater. Interfaces* **2018**, 10, 15428.
- [73] F. Xu, J. Zhu, L. Lin, C. Zhang, W. Sun, Y. Fan, F. Yin, J. C. M. van Hest, H. Wang, L. Du, X. Shi, *Theranostics* **2020**, 10, 4349.
- [74] P. Avcı, S. S. Erdem, M. R. Hamblin, *J. Biomed. Nanotechnol.* **2014**, 10, 1937.
- [75] X. Yi, J. Dai, Y. Han, M. Xu, X. Zhang, S. Zhen, Z. Zhao, X. Lou, F. Xia, *Commun. Biol.* **2018**, 1.
- [76] X. Yang, X. Shi, J. Ji, G. Zhai, *Drug Delivery* **2018**, 25, 780.
- [77] W. Hou, X. Zhao, X. Qian, F. Pan, C. Zhang, Y. Yang, J. M. De La Fuente, D. Cui, *Nanoscale* **2016**, 8, 104.
- [78] P. Mi, *Theranostics* **2020**, 10, 4557.
- [79] R. Augustine, D.-K. Kim, N. Kalva, K. H. Eom, J. H. Kim, I. Kim, *J. Mater. Chem. B* **2020**, 8, 5745.
- [80] Y. Dong, P. Du, P. Liu, *Int. J. Pharm.* **2020**, 588, 119723.
- [81] K. Kolouchova, O. Groborz, Z. Cernochova, A. Skarkova, J. Brabek, D. Rosel, P. Svec, Z. Starcuk, M. Slouf, M. Hruby, *Biomacromolecules* **2021**, 22, 2325.
- [82] X. Shi, Y. Zhang, Y. Tian, S. Xu, E. Ren, S. Bai, X. Chen, C. Chu, Z. Xu, G. Liu, *Small Methods* **2021**, 5, 2000416.
- [83] Q. Pan, J. Tian, H. Zhu, L. Hong, Z. Mao, J. M. Oliveira, R. L. Reis, X. Li, *ACS Biomater. Sci. Eng.* **2020**, 6, 2175.
- [84] F. Mastrotto, P. Caliceti, V. Amendola, S. Bersani, J. P. Magnusson, M. Meneghetti, G. Mantovani, C. Alexander, S. Salmaso, *Chem. Commun.* **2011**, 47, 9846.
- [85] C. Yan, Z. Guo, Y. Shen, Y. Chen, H. Tian, W. H. Zhu, *Chem. Sci.* **2018**, 9, 4959.
- [86] L. Hu, Q. Zhang, X. Li, M. J. Serpe, *Mater. Horiz.* **2019**, 6, 1774.
- [87] Y. Zou, D. Li, Y. Wang, Z. Ouyang, Y. Peng, H. Tomas, J. Xia, J. Rodrigues, M. Shen, X. Shi, *Bioconjugate Chem.* **2020**, 31, 907.
- [88] L. Zartner, M. S. Muthwill, I. A. Dinu, C.-A. Schoenenberger, C. G. Palivan, *J. Mater. Chem. B* **2020**, 8, 6252.
- [89] A. Napoli, M. Valentini, N. Tirelli, M. Muller, J. A. Hubbell, *Nat. Mater.* **2004**, 3, 183.
- [90] M. Karimi, P. Sahandi Zangabad, A. Ghasemi, M. Amiri, M. Bahrami, H. Malekzad, H. Ghahramanzadeh Asl, Z. Mahdih, M. Bozorgomid, A. Ghasemi, M. R. Rahmani Taji Boyuk, M. R. Hamblin, *ACS Appl. Mater. Interfaces* **2016**, 8, 21107.
- [91] D. Chandler, *Nature* **2005**, 437, 640.
- [92] Y. Mai, A. Eisenberg, *Chem. Soc. Rev.* **2012**, 41, 5969.
- [93] A. Bahri, M. Martin, C. Gergely, S. Marchesseau, D. Chevalier-Lucia, *Food Hydrocolloids* **2018**, 83, 53.
- [94] D. Lombardo, M. A. Kiselev, S. Magazu, P. Calandra, *Adv. Condens. Matter Phys.* **2015**, 2015, 151683.
- [95] P. van Rijn, M. Tutus, C. Kathrein, L. Zhu, M. Wessling, U. Schwaneberg, A. Boker, *Chem. Soc. Rev.* **2013**, 42, 6578.
- [96] S. Yadav, A. K. Sharma, P. Kumar, *Front. Bioeng. Biotechnol.* **2020**, 8, 127.
- [97] I. Ali, M. Alsehli, L. Scotti, M. Tullius Scotti, S. T. Tsai, R. S. Yu, M. F. Hsieh, J. C. Chen, *Polymers* **2020**, 12.
- [98] K. Kita-Tokarczyk, J. Grumelard, T. Haefele, W. Meier, *Polymer* **2005**, 46, 3540.
- [99] P. V. Pawar, S. V. Gohil, J. P. Jain, N. Kumar, *Polym. Chem.* **2013**, 4, 3160.
- [100] S. Allen, O. Osorio, Y. G. Liu, E. Scott, *J. Controlled Release* **2017**, 262, 91.
- [101] M. Karpuz, M. Silindir-Gunay, A. Y. Ozer, *Cancer Biother. Radiopharm.* **2018**, 33, 39.
- [102] Ö. Gezici, İ. Durmaz, E. Bilget Güven, Ö. Ünal, A. Özgün, R. Cetin-Atalay, D. Tuncel, *RSC Adv.* **2014**, 4, 1302.
- [103] M. A. Rahim, N. Jan, S. Khan, H. Shah, A. Madni, A. Khan, A. Jabar, S. Khan, A. Elhissi, Z. Hussain, H. C. Aziz, M. Sohail, M. Khan, H. E. Thu, *Cancers* **2021**, 13, 670.
- [104] Y. Liu, L. Feng, T. Liu, L. Zhang, Y. Yao, D. Yu, L. Wang, N. Zhang, *Nanoscale* **2014**, 6, 3231.
- [105] J. Di, X. Gao, Y. Du, H. Zhang, J. Gao, A. Zheng, *Asian J. Pharm. Sci.* **2021**, 16, 444.
- [106] Q. Zhou, L. Zhang, T. Yang, H. Wu, *Int. J. Nanomed.* **2018**, 13, 2921.
- [107] J. S. Suk, Q. Xu, N. Kim, J. Hanes, L. M. Ensign, *Adv. Drug Delivery Rev.* **2016**, 99, 28.
- [108] P. L. Turecek, M. J. Bossard, F. Schoetens, I. A. Ivens, *J. Pharm. Sci.* **2016**, 105, 460.
- [109] K. Wylon, S. Dölle, M. Worm, *Allergy, Asthma, Clin. Immunol.* **2016**, 12, 67.

- [110] G. T. Kozma, T. Mészáros, I. Vashegyi, T. Fülöp, E. Örfi, L. Dézsi, L. Rosivall, Y. Bavli, R. Urbanics, T. E. Mollnes, Y. Barenholz, J. Szebeni, *ACS Nano* **2019**, *13*, 9315.
- [111] C. A. Stone, Y. Liu, M. V. Relling, M. S. Krantz, A. L. Pratt, A. Abreo, J. A. Hemler, E. J. Phillips, *J. Allergy Clin. Immunol.: Pract.* **2019**, *7*, 1533.
- [112] F. Cox, K. Khalib, N. Conlon, *J. Clin. Pharmacol.* **2021**, *61*, 832.
- [113] C. Domingues, C. Alvarez-Lorenzo, A. Concheiro, F. Veiga, A. Figueiras, *Mol. Pharmaceutics* **2019**, *16*, 4757.
- [114] M. Garni, R. Wehr, S. Y. Avsar, C. John, C. Palivan, W. Meier, *Eur. Polym. J.* **2019**, *112*, 346.
- [115] Y. Wang, M. S. Shim, N. S. Levinson, H. W. Sung, Y. Xia, *Adv. Funct. Mater.* **2014**, *24*, 4206.
- [116] M. Mohammadi, M. Ramezani, K. Abnous, M. Alibolandi, *Int. J. Pharm.* **2017**, *519*, 287.
- [117] C. Edlinger, T. Einfalt, M. Spulber, A. Car, W. Meier, C. G. Palivan, *Nano Lett.* **2017**, *17*, 5790.
- [118] L. Zartner, V. Maffei, C.-A. Schoenenberger, I. A. Dinu, C. G. Palivan, *J. Mater. Chem. B* **2021**, *9*, 9012.
- [119] C. D. G. Abueva, *Med Laser* **2021**, *10*, 7.
- [120] A. A. Halwani, *Pharmaceutics* **2022**, *14*, 106.
- [121] T. Cele, in *Engineered Nanomaterials - Health and Safety*, IntechOpen, **2020**.
- [122] T. Saeed, A. Naem, T. Mahmood, N. Huma Khan, in *Engineered Nanomaterials - Health and Safety*, IntechOpen, **2020**.
- [123] S. Kango, S. Kalia, A. Celli, J. Njuguna, Y. Habibi, R. Kumar, *Prog. Polym. Sci.* **2013**, *38*, 1232.
- [124] W. Xie, Z. Guo, L. Zhao, Y. Wei, *Theranostics* **2021**, *11*, 6407.
- [125] S. Mourdikoudis, R. M. Pallares, N. T. K. Thanh, *Nanoscale* **2018**, *10*, 12871.
- [126] H. Zhou, J. Ge, Q. Miao, R. Zhu, L. Wen, J. Zeng, M. Gao, *Bioconjugate Chem.* **2020**, *31*, 315.
- [127] Y. Zhong, Y. Zou, L. Liu, R. Li, F. Xue, T. Yi, *Acta Biomater.* **2020**, *115*, 358.
- [128] X. Ge, Q. Fu, L. Su, Z. Li, W. Zhang, T. Chen, H. Yang, J. Song, *Theranostics* **2020**, *10*, 4809.
- [129] S. R. Sershen, S. L. Westcott, N. J. Halas, J. L. West, *J. Biomed. Mater. Res.* **2000**, *51*, 293.
- [130] J. He, X. Huang, Y. C. Li, Y. Liu, T. Babu, M. A. Aronova, S. Wang, Z. Lu, X. Chen, Z. Nie, *J. Am. Chem. Soc.* **2013**, *135*, 7974.
- [131] D. Wang, N. Zhang, T. Yang, Y. Zhang, X. Jing, Y. Zhou, J. Long, L. Meng, *Acta Biomater.* **2022**, *147*, 245.
- [132] P. G. van Rhee, R. S. Rikken, L. K. Abdelmohsen, J. C. Maan, R. J. Nolte, J. C. van Hest, P. C. Christianen, D. A. Wilson, *Nat. Commun.* **2014**, *5*, 5010.
- [133] H. F. Gilbert, *Adv. Enzymol. Relat. Areas Mol. Biol.* **1993**, *63*, 69.
- [134] W. Zhuang, B. Ma, J. Hu, J. Jiang, G. Li, L. Yang, Y. Wang, *Theranostics* **2019**, *9*, 6618.
- [135] R. Augustine, D. K. Kim, S. H. Jeon, T. W. Lee, N. Kalva, J. H. Kim, I. Kim, *React. Funct. Polym.* **2020**, *152*, 104595.
- [136] J. Y. Yhee, S. Son, S. H. Kim, K. Park, K. Choi, I. C. Kwon, *J. Controlled Release* **2014**, *193*, 202.
- [137] H. P. Chen, M. H. Chen, F. I. Tung, T. Y. Liu, *J. Med. Chem.* **2015**, *58*, 3704.
- [138] C. You, Z. Gao, H. Wu, K. Sun, L. Ning, F. Lin, B. Sun, F. Wang, *J. Mater. Chem. B* **2019**, *7*, 314.
- [139] A. Belluati, I. Craciun, J. Liu, C. G. Palivan, *Biomacromolecules* **2018**, *19*, 4023.
- [140] R. Xiong, S. J. Soenen, K. Braeckmans, A. G. Skirtach, *Theranostics* **2013**, *3*, 141.
- [141] C. E. Meyer, S. L. Abram, I. Craciun, C. G. Palivan, *Phys. Chem. Chem. Phys.* **2020**, *22*, 11197.
- [142] X. Yang, J. Xiong, P. C. Qiu, M. Chen, D. G. He, X. X. He, K. M. Wang, J. L. Tang, *RSC Adv.* **2017**, *7*, 7742.



**Moritz S. Muthwill** is a pharmaceutical scientist from University Freiburg, Germany, in 2019, with background in biotechnology and toxicology. He is currently a Ph.D. candidate in Cornelia Palivan's group in the Department of Chemistry, University of Basel, Switzerland, with focus on development of biomimicking polymeric "smart" membranes for application in biomedicine and life sciences.



**Phally Kong** is a polymer chemist who obtained her bachelor's and master's degree in molecular and biological chemistry at the Swiss Federal Institute of Technology of Lausanne (EPFL). She pursued her Ph.D. degree in the Department of Chemistry at the University of Fribourg, Switzerland, in polymer chemistry focusing on the design, synthesis, and the physical property of polymers. She then joined within the group of Meier/Palivan at the University of Basel as a postdoctoral fellow in synthesis and characterization of pH-responsive block copolymers and investigation on their stimuli-responsiveness through nanoself-assemblies in solution and on giant unilamellar vesicles via microfluidics.



**Ionel Adrian Dinu** received his Ph.D. in macromolecular chemistry at the “P. Poni” Institute of Macromolecular Chemistry, Iasi, Romania, in 2010. In 2012, he joined the group of Prof. Wolfgang Meier as a postdoc, at the University of Basel, Switzerland, and he is currently senior scientific collaborator at the same university. His main research is focused on the design of amphiphilic block copolymers and fabrication of (bio-) functional polymer nanostructures via hierarchical self-assembly.



**Cornelia G. Palivan** studied physics at the University of Bucharest and received her Ph.D. degree in 1995, after a two-year research stage at the University of Geneva. In 1999 she joined the Department of Chemistry at the University of Basel where she currently is professor in physical chemistry. She received several awards for her research. Previously focused on structural characterization of metal complexes with biologic activity, she enlarged her domain of interest by development of multifunctional hybrid systems and materials.